The transport mechanism of the mitochondrial ADP/ATP carrier

Edmund R.S. Kunji*, Antoniya Aleksandrova, Martin S. King, Homa Majd, Valerie L. Ashton, Liz Cerson, Roger Springett, Mikhail Kibalchenko, Sotiria Tavoulari, Paul G. Crichton, and Jonathan J. Ruprecht

The Medical Research Council, Mitochondrial Biology Unit, Cambridge Biomedical Campus, Wellcome Trust / MRC Building, Hills Road, Cambridge, CB2 0XY, UK.

*Correspondence: Edmund R.S. Kunji, ek@mrc-mbu.cam.ac.uk

Abstract

The mitochondrial ADP/ATP carrier imports ADP from the cytosol and exports ATP from the mitochondrial matrix, providing key steps in oxidative phosphorylation in eukaryotic organisms. The transport protein belongs to the mitochondrial carrier family, a large transporter family in the inner membrane of mitochondria. It is one of the best studied members of the family and serves as a paradigm for the molecular mechanism of mitochondrial carriers. Structurally, the carrier consists of three homologous domains, each composed of two transmembrane α-helices linked with a loop and short α-helix on the matrix side. The transporter cycles between a cytoplasmic and matrix conformation in which a central substrate binding site is alternately accessible to these compartments for binding of ADP or ATP. On both the cytoplasmic and matrix side of the carrier are networks consisting of three salt bridges each. In the cytoplasmic conformation, the matrix salt bridge network is formed and the cytoplasmic network is disrupted, opening the central substrate binding site to the intermembrane space and cytosol, whereas the converse occurs in the matrix conformation. In the transport cycle, tighter substrate binding in the intermediate states allows the interconversion of conformations by lowering the energy barrier for disruption and formation of these networks, opening and closing the carrier to either side of the membrane in an alternating way. The simultaneous

rotation of three domains around a central translocation pathway constitutes a unique mechanism among transport proteins.

Keywords: adenine nucleotide translocator, adenine nucleotide translocase, transport protein, transport mechanism, alternating access mechanism.

Abbreviations

AAC1 bovine mitochondrial ADP/ATP carrier isoform 1; Aac2p; yeast mitochondrial ADP/ATP carrier isoform 2; Aac3p; yeast mitochondrial ADP/ATP carrier isoform 3; ATR atractyloside; CATR carboxyatractyloside; BKA bongkrekic acid; AFM atomic force microscopy; NMR nuclear magnetic resonance; CPM N-[4-(7-diethylamino-4-methyl-3-coumarinyl)-phenyl]-maleimide

Introduction

The mitochondrial ADP/ATP carrier is one of the most abundant proteins of the mitochondrial inner membrane. The activity of the carrier is the first and last step in oxidative phosphorylation in eukaryotic organisms, as it exports ATP, synthesised by ATP synthase, out of the mitochondrion for use in the cytosol and imports the spent fuel ADP back into the mitochondrion for ATP synthesis (Figure 1). It is estimated that our own body weight in ADP and ATP is transported every day by these carriers to sustain the energy-requiring processes in the cells of the human body. The ADP/ATP carrier belongs to the mitochondrial carrier family of membrane proteins, along with many other members that exchange various metabolites in and out of mitochondria [1]. As it is the most abundant carrier in the mitochondrial inner membrane, it is one of the best studied members of the transporter family.

Figure 1. Mitochondrial ATP synthase and the ADP/ATP and phosphate carriers.

The mitochondrial ADP/ATP carrier was discovered in the early sixties by the Klingenberg [2, 3] and Vignais [4] laboratories, following studies with the specific inhibitor atractyloside (ATR), which was known to inhibit respiration [5]. It was shown that ADP/ATP exchange is controlled by the proton electrochemical gradient

[6]. Since one ADP, which has three negative charges, is exchanged for one ATP, which has four negative charges, the equimolar exchange is electrophoretic, driven by the membrane potential [7, 8], which leads to a higher ATP phosphorylation potential in the cytosol than in mitochondria [9].

Another major advance came from the discovery of a second specific inhibitor, bongkrekic acid (BKA) [10]. It could be demonstrated that ATR and BKA binding have opposite effects on the carrier with respect to adenine nucleotide efflux [11]. Atractyloside, and the related inhibitor carboxyatractyloside (CATR) [12, 13], bind to the cytoplasmic conformation when the substrate binding site is exposed to the intermembrane space, and via channels to the cytosol. In contrast, BKA, and the related isobongkrekic acid [14], bind to the matrix conformation [11, 15]. These observations gave rise to the "single binding centre gated pore mechanism" [15, 16], which in essence is an alternating access mechanism, as first proposed for the P-type ATPase [17]. The isolation of the CATR-bound complex in Triton X-100 [18, 19] allowed the first reconstitution experiments of a transport protein to be carried out [20]. Thus, the main role of the mitochondrial ADP/ATP carrier is to exchange one ADP for one ATP molecule by an electrophoretic mechanism [21, 22]. Most eukaryotic organisms have several isoforms to allow control of this important function. Yeast, for example, has three isoforms of the ADP/ATP carrier, Aac1p [23], Aac2p [24] and Aac3p [25]. Aac2p is the principal ADP/ATP carrier expressed in aerobically growing yeast, whereas Aac1p is only expressed at low levels [26, 27]. Aac3p is expressed almost exclusively under anaerobic growth conditions [25], where it is thought to transport ATP produced by glycolysis into the mitochondrion [28]. In man there are four isoforms, AAC1 [29], AAC2 [30, 31], AAC3 [32] and AAC4 [33]. The AAC1 gene is expressed abundantly in heart, skeletal muscle, lung and testis and in lower amounts in brain, kidney, liver, pancreas and small intestine; the AAC2 gene is expressed at higher levels in lung, testis and small intestine and less in kidney, liver and pancreas; the AAC3 gene is expressed ubiquitously but in very abundant amounts in lung and testis and strongly in pancreas and small intestine, whereas AAC4 is expressed at low levels in lung and testis [33]. There are no obvious functional differences between these isoforms, and so the main reason for different isoforms might be for genetic control of the expression levels in response to

different energetic requirements. Since ADP/ATP carriers are only capable of equimolar exchange, mitochondria have ATP-Mg/Pi carriers to alter the adenine nucleotide pools in response to calcium [34-36].

Sequence, toplogy and structure

The complete amino acid sequence of the bovine ADP/ATP carrier was determined by Klingenberg [37], providing the first sequence of a mitochondrial carrier protein. It was noted by Saraste and Walker that there are three homologous sequence repeats [38], which was found to be a defining feature of mitochondrial carriers, when more sequences of mitochondrial carriers became available [39-42]. Another key sequence feature was the signature motif of the mitochondrial carrier family PX[DE]XX[KR], which can be found at the end of the odd-numbered α-helices in all three repeats [43]. A topology model for the mitochondrial carrier was proposed [44], consisting of six transmembrane α-helices with the N- and C-terminal ends both in the intermembrane space [45-48]. Using secondary structure predictions and analysis of conservation, this model was refined by extending the length of the odd-numbered α-helices to include the signature motifs and by adding short α-helices in the matrix loops [49, 50] (Figure 2). As will be discussed later, there are other well-conserved symmetrical features in mitochondrial carriers that are important for the mechanism.

Figure 2 Topology model of the yeast ADP/ATP carrier Aac3p.

The ADP/ATP carrier functions as a monomer

Elucidating the tertiary structure of a protein is a key step in understanding its mechanism. For almost 35 years the general consensus had been that mitochondrial ADP/ATP carriers are dimeric in structure and function. This view was based on data from inhibitor binding studies [18, 51], small-angle neutron scattering [52], freeze-fracture electron microscopy [53], size exclusion chromatography [54], analytical ultracentrifugation [54], blue native gel electrophoresis [55-58], cross-linking experiments [59-61], and tandem-fusions of active and inactive carriers [62, 63]. Two models were proposed; (i) a dimer with the translocation path between two

protomers [62], consistent with a ping-pong mechanism [64], or (ii) a dimer consisting of interacting protomers in opposing conformations [65], consistent with a simultaneous mechanism [66]. However, these models were no longer tenable when the first structural information became available.

Figure 3 Projection structure of the yeast mitochondrial ADP/ATP carrier Aac3p by electron crystallography.

The projection structure of the yeast ADP/ATP carrier Aac3p in complex with ATR, solved by electron crystallography, showed that the protein in the membrane was a structural monomer with six transmembrane α-helices arranged with three-fold pseudo-symmetry [49] (Figure 3), consistent with the three homologous sequence repeats [38] (Figure 2). The translocation path for adenine nucleotides was clearly through the centre of the protein. These features were at odds with the proposed dimer models, and thus it was suggested, for the first time, that mitochondrial ADP/ATP carriers could function as monomers [49]. There were two asymmetric features in the projection map, one strong and one weak, which were difficult to assign at the time (Figure 3). Recently, the structure of the same protein in complex with CATR was solved by x-ray crystallography, providing an atomic model for the interpretation of the projection map [67]. The strong density feature is likely to be ATR and the weak one a short α-helical extension of the first transmembrane helix at the matrix side (see also below) (Figure 3).

The atomic structures of the bovine AAC1 first [68] and the yeast Aac2p and Aac3p later [67] confirmed a monomeric structural fold. Crystallographic dimers were present in the projection map of yeast Aac3p [49], in one crystal form of the bovine carrier [69] and in several crystal forms of the yeast carriers [67]. However, in all cases the interaction interfaces were small and involved only cardiolipin molecules or non-conserved residues, which is incompatible with homo-dimerisation [67]. Other analysis has demonstrated that the yeast ADP/ATP carriers were monomeric in detergents when assessed by size exclusion chromatography [70], analytical ultracentrifugation [70], differential tagging and affinity purification [71], blue native electrophoresis [72], and, most recently, by multi-angle laser light

scattering (Jonathan Ruprecht, Liz Cerson and Martin King, unpublished data). The bovine ADP/ATP carrier was also shown to be monomeric in detergent by analytical ultracentrifugation [73]. When the yeast ADP/ATP carrier Aac3p was reconstituted in membranes at lower protein/lipid ratios than those used for two-dimensional crystals [49], only small crystalline patches and single protein molecules were observed by atomic force microscopy [74]. Furthermore, transport assays with co-expressed sulfhydryl sensitive and insensitive yeast ADP/ATP carriers demonstrated that the carriers function as monomers in the mitochondrial membrane [75].

But what about the earlier claims for a dimer? Determining the oligomeric conformation of membrane proteins is technically challenging, especially since these proteins are small, hydrophobic and very unstable in detergent. In sizing techniques, such as size exclusion chromatography, analytical centrifugation, and blue native electrophoresis, it is crucial to account for the contribution of the lipid/detergent micelle to the total mass, which is much bigger than the contribution of the carrier protein [70, 76]. With the advantage of hindsight all of the inconsistencies could be explained (see [77] for a retrospective analysis), providing further support for the monomer being the functional unit. The uncoupling protein, which is belongs to the mitochondrial carrier family, is also a monomer [78]. Recently, we have characterised the mitochondrial aspartate/glutamate carrier, another family member, which has proved to be a structural homo-dimer. Here, dimerisation is mediated by additional N-terminal domains consisting of EF-hands that form an extensive interaction interface, but importantly the carrier domains themselves do not dimerize [79]. Thus the mitochondrial ADP/ATP carrier functions as a monomer.

The atomic structures of the bovine and yeast ADP/ATP carrier

The first atomic structure to be determined was that of the bovine ADP/ATP carrier AAC1 in complex with CATR [68] (Figure 4A). The structure revealed the structural fold of the protein locked in the cytoplasmic conformation by the inhibitor. The six transmembrane α-helices are highly tilted and form an α-helical barrel around a water-filled cavity. Three short α-helices on the matrix side of the carrier run roughly parallel with the membrane plane and connect the odd and even-numbered α-helices (Figure 4A). The structure has three-fold pseudo-symmetry in agreement

with the three sequence repeats [38] and the projection structure of Aac3p [49] (Figure 4A). The atomic structures of yeast Aac2p and Aac3p have a very similar fold (Figure 4B), confirming the basic structure consisting of three similar domains (primary colours Figure 4) [67].

Figure 4 Architecture of the bovine and yeast ADP/ATP carrier by x-ray crystallography.

There are a few differences between the yeast and bovine structures. First, the extreme C-terminal region of the yeast carriers folds back into the central cavity as a loop, which is absent in the bovine carrier (Figure 4B). Second, the yeast carriers have an extra helical turn at the end of the first transmembrane helix H1, which is a loop in the bovine carrier. Third, the N-terminal region of the first transmembrane helix H1 of Aac3p extends into the intermembrane space by another three helical turns compared to the bovine carrier (Figure 4A and B). In contrast, Aac2p is predicted to have an N-terminal loop region of 22 amino acid residues, but this sequence was deleted in the construct used for crystallography.

Figure 5 CATR binding to the yeast mitochondrial ADP/ATP carrier Aac3p.

All atomic structures were solved in complex with CATR, as it confers a remarkable increase in stability of the protein [18, 70] (see also below). The CATR molecule is bound asymmetrically in the central cavity [67, 68]. In the yeast structures CATR was modelled with a β-D-glucoside ring [67] (Figure 5), rather than the α-D-glucoside in the bovine structure [68, 69]. A β-D-glucoside ring is consistent with the crystal structure of ATR [80] and NMR studies of CATR and ATR [81]. CATR differs from ATR by one carboxylate group that gives extra resistance to unfolding of yeast Aac3p by single-molecule force spectroscopy, which was located to transmembrane H2, again consistent with a β-D-glucoside ring [80, 81].

Figure 6 Proline and serine residues in the signature motifs of Aac2p.

It was noted first in the bovine structure that the odd-numbered α-helices have a pronounced L-shape [68]. The symmetrically conserved proline residues of the signature motif PX[DE]XX[RK] are found at the kink in these helices. Similar kinks are found in the odd-numbered α-helices of the yeast carriers (Figure 6A), even though the proline residue in transmembrane H3 is replaced by a serine (Figure 6B). The hydroxyl group of the serine forms an interaction with its own backbone nitrogen, mimicking a proline residue. The proline and serine residues allow the kink to occur, because the hydrogen bonding arrangement of the helix is interrupted (Figure 6), but the kink itself is stabilised by interactions with other residues of the domain, including the matrix α-helices [67].

Figure 7 Cardiolipin binding site of the yeast ADP/ATP carrier.

Cardiolipin binding to the ADP/ATP carrier

Phosphorous NMR experiments have shown previously that cardiolipin molecules are tightly bound to the ADP/ATP carrier [82]. Impairment of cardiolipin synthesis in yeast still allows growth on non-fermentable carbon sources, indicating that the carrier is still functional [83], but in man it leads to Sengers syndrome, in which the carrier disappears from the inner membrane, leading to a severe oxidative phosphorylation disease phenotype [84, 85]. Three tightly bound cardiolipin molecules were found in the structure of the bovine ADP/ATP carrier [68, 69]. The phosphate groups were hydrogen bonded to the N-terminal ends of the even-numbered and matrix α-helices, spanning the inter-domain interface. The yeast structures also contained three bound cardiolipins arranged in a similar manner (Figure 7A) [67]. By analysing 27 available cardiolipin binding sites from the crystal structures we made several observations that may explain why these lipid molecules are bound so tightly. First, preceding the even-numbered and matrix α-helices are the conserved symmetrical sequence motifs [YWF][RK]G and [YF]XG, respectively. The glycine residues of these motifs are in the loop to helix transition, as they function as helix breakers. As a consequence, the amide groups at the start of the α-helices do not have hydrogen bonding partners, and thus the phosphate groups of

cardiolipin may act as hydrogen bond acceptors. Second, the bound cardiolipin molecules are most likely to have two formal negative charges [86], because the central hydroxyl group does not form a hydrogen bond with either of the two phosphate moieties (Figure 6B). The charged head groups of cardiolipin are bound in a hydrophobic environment and thus there has to be a charge compensation mechanism, but the positively charged residues of the [YWF][RK]G motif do not interact directly with the phosphate groups with one possible exception. However, the N-terminal ends of the even-numbered and matrix α-helices will have a positive charge from the helix dipole, which may interact electrostatically with the negatively charged phosphate moieties of cardiolipin. Thus the three cardiolipin molecules are most likely bound by several hydrogen bonds and by electrostatic interactions (Figure 7) [67].

Figure 8 Yeast ADP/ATP carriers in the membrane – molecular dynamics simulations and atomic force microscopy.

The position of the ADP/ATP carrier in the membrane

Several molecular dynamics (MD) studies have been done with the bovine ADP/ATP carrier [87-89] and the yeast ADP/ATP carrier Aac2p (Antoniya Aleksandrova, unpublished data), which have shown a consistent pose in the membrane. The cytoplasmic side of the carrier is virtually flush with the surface of the membrane (Figure 8), showing only the central cavity as a hole (Figure 8A). The matrix side protrudes from the membrane by 7-10 Å and thus the matrix side can be seen on the surface (Figure 8B). These observations agree well with high-resolution AFM topographs of the two-dimensional crystals, similar to those shown in Figure 2 (Figure 8). The crystals consist of rows of Aac3p crystallographic dimers with alternating orientations as can be clearly seen in the AFM topograph [74] (Figure 8C). The measured difference in height between the differently oriented rows of Aac3p is ~7 Å, which agrees well with the available atomic structures [67, 68].

Identification of the substrate binding site of the ADP/ATP carrier

The ADP/ATP carrier has a very strict substrate specificity, as was noted first for the bovine ADP/ATP carrier [6]. Recently, the substrate specificity of the human carrier was determined [89]. Remarkably, only ADP and ATP and their deoxy variants are transported. Thus the commonly used names adenine nucleotide translocase or translocator would appear to be misnomers, as neither AMP nor any other adenine nucleotides are transported.

Figure 9 Different approaches used for identification of the substrate binding site.

Three independent approaches have been applied to locate the substrate binding site. The first approach used comparative structural models combined with chemical and distance constraints to identify conserved sites that were capable of discriminating between different amino and keto acid substrates of mitochondrial carriers [90, 91]. It was anticipated that the models may not be correct, and thus the distance restraints were applied loosely. These searches located a unique site that could explain the specificity of known transporters. The main contact points involved in substrate binding were located on the even-numbered α-helices. Inspection of the same site in the ADP/ATP carrier showed that it was also able to bind adenine nucleotides. On this basis it was proposed that the substrate binding site of bovine AAC1 consisted of G182, I183 and Y186 for binding of the adenine moiety and R79, K22 and R279 for binding of the phosphate groups [90, 91] (Figure 9A).

The second approach exploited the principle that mitochondrial carriers have a high degree of three-fold symmetry [38], whereas the transported substrates are asymmetric in structure and chemistry [92]. Therefore, the carriers must have evolved asymmetric substrate binding sites as adaptations to the asymmetric substrates. Based on sequence information only, a score was devised to assess the degree of symmetry and conservation of all residues in mitochondrial carriers [92]. For all known subfamilies of mitochondrial carriers conserved asymmetric residues were found to cluster consistently at a site that overlapped with the substrate binding site mentioned above [90, 91]. Importantly, no other clusters of asymmetric residues were found on the water-accessible surfaces of the carriers, indicating that mitochondrial carriers have a single substrate binding site. For the ADP/ATP carrier

the cluster of asymmetric residues was more extensive, but involved the asymmetric residues G182, Y186, S227 and K22 and the symmetric residues R79 and R279, which potentially allow coupling to a symmetric transport mechanism (Figure 9B). In addition, there are asymmetric polar residues on the cytoplasmic side (K91 and N87) and matrix side (R235 and T138) (see below).

The third approach used molecular dynamics simulations to identify residues of the bovine mitochondrial ADP/ATP carrier that are involved in the trajectory and binding of ADP in the cavity [87, 89, 93]. Although ADP binds in many places along the trajectory, two consensus sites emerged from these three studies. The first site involves the aforementioned residues, but the β-phosphate binds to R235 (Figure 9C). The second involves residues R79, R279 and R235 for binding of the phosphate moieties, and K22, S21 and A284 for binding of the adenine moiety (Figure 9D).

A consensus for the central substrate binding site emerges from comparison of the three approaches, which is shown in the yeast Aac2p with a modelled substrate (Figure 10). The adenine moiety has an aromatic stacking arrangement with Y203, hydrophobic interactions with G199 and I200, and a hydrogen bond with S245 (Y186, G182, I183, and S227 in bovine AAC1, respectively). The hydroxyl group of the Y203 might form a hydrogen bond with the hydroxyl group of the ribose. As depicted, the phosphate groups of ATP are bound to K38, R96, and R294, which leaves one net negative charge. If ADP is bound to the same site in a similar way, the substrate would be neutralised. This notion is consistent with an electrophoretic or electrogenic exchange [21, 22], as there would be a net negative charge difference.

Figure 10 Proposed substrate binding site of the mitochondrial ADP/ATP carrier.

What about the other charged asymmetric residues in the cavity, K91 and R235 in AAC1 (Figure 9B)? The molecular dynamics studies have shown that in the cytoplasmic conformation R235 is involved in binding of β-phosphate [87, 89, 93]. In this way binding of the terminal phosphate might hold the highly flexible ADP molecule in a pose that would lead to the disruption of the matrix network. Residue K91 may fulfil a similar role for the binding of ATP when the carrier is in the matrix conformation. These additional intermittent interactions could explain the charges

of −0.7 and +0.3 upon binding of ATP and ADP, respectively, in direct measurement of electrical currents of ADP/ATP transport [64]. The location of the substrate binding site is supported also by the observation that the photo-activated ADP analogue 2- azido[α-^{32}P]adenosine diphosphate reacts with I183 in AAC1 [94]. The tyrosine residue (Y186 in AAC1), involved in an aromatic stacking arrangement with the adenine ring, is also critical for the function of the carrier [95].

The proposed substrate binding site has several interesting properties. The location corresponds approximately to the middle of the membrane, as observed for other transporters. The water-filled cavity allows the substrate to move to the middle of the membrane, which is energetically the most unfavourable position for a charged and polar substrate. The site could function as a pivot point for conformational changes, allowing the alternating access of the site to either side of the membrane. The main contact points I, II and III of the common substrate binding site are located on the even numbered α-helices H2, H4 and H6, respectively, which are related by three-fold pseudo-symmetry allowing the binding of the substrate to be coupled to a common structural mechanism of transport (Figure 10).

Figure 11 Main functional elements of the mitochondrial ADP/ATP carrier.

Salt bridge networks of the mitochondrial ADP/ATP carrier

The structure of the bovine AAC1 showed that the charged residues of the signature motif PX[DE]XX[RK] form a salt bridge network on the matrix side when the carrier is in the cytoplasmic conformation [68]. Formation and disruption of this salt bridge network had previously been proposed on the basis of second-site revertants [43]. A similar arrangement can be observed in the structures of the yeast Aac2p and Aac3p (Figure 10), but we noticed that in one domain a glutamine residue forms hydrogen bonds with both residues of the salt bridge [67]. Equivalently arranged glutamine residues could be present in other mitochondrial carriers, as they are highly conserved, but their number per protein varies, indicating different adaptations to function. We have called this interaction the glutamine brace, which serves to increase the overall interaction energy of the matrix network.

Our analysis of the carrier symmetry revealed a highly conserved and symmetrical [FY][DE]XX[RK] motif on the cytoplasmic side of the carrier (Figure 11), which also has the propensity to form a salt bridge network [92]. These residues are located on the even-numbered α-helices, whereas the residues of the matrix network are on the odd-numbered α-helices. In the cytoplasmic state these residues are not engaged in interactions [67], so it was proposed that the network forms in the matrix conformation. Both networks align with the water-membrane interface at either side of the carrier, where solute access to the central substrate binding site may be controlled by closing and opening of the carrier to either side of the membrane. Based on these functional features, we proposed an alternating access mechanism of substrate exchange by the carriers (Figure 12) [92]. In the mechanism, substrate binding in one conformation allows the conversion to the other conformation by the disruption and formation of these networks, causing the alternating opening and closing of the carrier to either side of the membrane. The high interaction energies of the two networks will prevent the interconversions between conformations in the absence of substrate, which would account well for the observed equimolar exchange of ADP and ATP. Semi-quantitatively, the interaction energies involved in substrate binding and formation of the salt bridge networks are balanced, which allow the interconversions of states to occur [96].

Figure 12 Proposed transport mechanism of the mitochondrial ADP/ATP carrier.

Only recently have we been able to provide experimental support for the formation of the cytoplasmic network. First it was shown that the charges of the cytoplasmic salt bridge network are crucial for the transport cycle [67]. Residues of the proposed cytoplasmic network were mutated to engineer networks with only positively charged residues, only negatively charged residues, or with residues that had the opposite charge of those of the wild-type carrier. Mutant carriers with all positively or all negatively charged residues (three mutations each) were not active, as the same charge opposed their interactions. However, the mutant with the charged residues of the cytoplasmic network interchanged (six mutations in total) was active, albeit to only 14% of the wild-type rate. This result indicated that the cytoplasmic

network must form as part of the transport cycle, though it does not prove that it forms in the matrix state. To demonstrate this, we have developed a new approach that combines mutagenesis with protein thermostability measurements based on the thiol-reactive CPM probe. CPM forms a blue fluorescent adduct after reaction with an exposed protein thiol (Figure 13A). The probe was used in an assay in the Stevens lab to test the relative stability of membrane proteins to aid crystallisation trials [97], but we have adapted the assay and developed it as a powerful tool to obtain key biological information. In the procedure, the temperature of purified protein samples is increased from 25 to 90 °C, buried cysteine residues become solvent exposed due to thermal denaturation of the protein and an unfolding curve is obtained through fluorescence measurements [98]. The peak in the derivative of the unfolding curve, the "melting temperature", provides a relative measure of protein stability. We have used the assay to provide information on detergent, lipid, substrate and inhibitor interactions with various mitochondrial carriers and uncoupling proteins [78, 96, 98].

Figure 13 Thermostability of purified wild-type ADP/ATP carrier in detergent in the presence of inhibitors and ADP.

The assay has also been used to study the conformations of the ADP/ATP carrier of the thermophilic fungus *Myceliophthora thermophile*, which is more stable in detergent in the unliganded form [96]. The unfolding profiles of the wild-type carrier were determined in the absence or presence of CATR or BKA (Figure 13B and C). As the binding of these inhibitors is state-dependent, it was necessary to also add the substrate ADP in small amounts to allow cycling between states to obtain one inhibited population [15, 16, 96]. In the absence of inhibitor, the carrier had a relatively low apparent melting temperature of ~50 °C. Addition of CATR resulted in a 33 °C increase in the apparent melting temperature of the carrier, whereas addition of BKA only led to an 11 °C increase (Figure 13A and B). Remarkably, a raised baseline was observed in the presence of BKA, indicating that one of two cysteine residues in the protein had become exposed (Figure 13A). Mutagenesis demonstrated that this cysteine residue belongs to a highly conserved [DE]C motif in

the matrix α-helices [96], which is also the target of sulfhydryl reagents [75] and cross-linking under oxidising conditions [59-61], but only when the carrier is in the BKA-inhibited conformation. Thus the CPM assay can be used to distinguish the conformations of the ADP/ATP carrier. CATR is bound to the central cavity by an extensive network of salt bridges, hydrogen bonds and hydrophobic contacts, cross-linking most of the transmembrane α-helices, which could easily account for the large increase in stability (Figure 5). Although it is not known how BKA binds, it is a relatively long and flexible molecule with only three carboxylic groups, providing fewer and weaker binding opportunities than CATR, consistent with these results.

Figure 14 Cytoplasmic salt bridge network of the mitochondrial ADP/ATP carrier

The cytoplasmic salt bridge network forms in the matrix state

Since the conformation of the carrier can be defined by the CPM assay, we used it to study the effect of mutations of the cytoplasmic network on the matrix and cytoplasmic conformation [96]. A series of mutations were introduced with the aim to increase or decrease the overall interaction energy of the cytoplasmic network of the ADP/ATP carrier. Previously, we have introduced a semi-quantitative measure for the interaction energy of these networks by counting the number of potential salt bridge and hydrogen bond interactions, assuming that hydrogen bonds have about half the interaction energy of a salt bridge [92]. On this basis the cytoplasmic network of the wildtype has a putative interaction energy of 2.5, based on two salt bridges and one hydrogen bond (Figure 14). By introducing mutations, the interaction energy of the cytoplasmic network was varied from 3.0 to 0.5 (Figure 14). Next the mutant and wild-type carriers were purified, and the effect of the mutations on the thermostability was determined when the carriers were locked in either the cytoplasmic or the matrix state with CATR plus ADP or BKA plus ADP, respectively. The thermostability of the unliganded or CATR-inhibited carrier was unaffected by the mutations, whereas the thermostability of BKA-inhibited carrier correlated with the interaction energy of the cytoplasmic salt bridge network, demonstrating the formation of the cytoplasmic network in that state (Figure 15).

The data also support the notion that the salt bridge interactions of the cytoplasmic network form simultaneously [96].

Figure 15 Thermostability of the BKA-inhibited conformation is dependent on the interaction energy of the cytoplasmic network.

Towards a structural model of the alternating access mechanism

Currently there is no structural model of the matrix conformation, which hampers our ability to understand the transport mechanism. Careful analysis of the polar interactions in the bovine and yeast structures has shown that there are more interactions within the domains than between the domains [67]. The most significant and conserved inter-domain interactions are the salt bridge networks, which clearly have a defined functional role. Most of the intra-domain interactions are on the matrix side of the carrier, cross-linking the matrix and transmembrane α-helices together. On the cytoplasmic side are many aromatic residues that may stabilise the domain structure through aromatic interactions and there are very few polar interactions between the α-helices. Thus, it is likely that the conformational changes involve domain movements as rigid bodies.

Figure 16 Conserved properties of the inter-domain interfaces suggest a domain-based mechanism of transport.

The movements of the domains as part of the transport cycle are not known, but inspection of the inter-domain surfaces provided some clues [67]. Normally, the side chains of the inter-helical interfaces interact in a "lock and key" manner, but that is not the case for the inter-domain interfaces of the ADP/ATP carrier. The surface of the inter-domain interfaces on the odd-numbered α-helices consists almost entirely of residues with no or small side chains, except for the cytoplasmic ends (Figure 16A). Among them are glycine residues of the well-conserved symmetrical sequence motif GXXXG, which are on the same face of the helix and are important for function [99]. These motifs are commonly found in membrane proteins in regions of close inter-helical contact [100]. On the even-numbered α-

helices, hydrophobic residues face the membrane whereas hydrophilic residues face the cavity, neither pointing towards the interface except for a few small residues (Figure 16B. This analysis indicated that the inter-domain interfaces are relatively smooth, suggesting that the even-numbered α-helices may move across the surface of the odd-numbered α-helices, during the domain motions (Figure 16C). There are many possibilities for the motions of the domains, but in the cytoplasmic to matrix transition the cytoplasmic salt bridge network must form in the matrix state, which indicates rotation of the domains into the centre (Figure 16C).

Conclusions

In this review we have described recent progress towards a transport mechanism for the mitochondrial ADP/ATP carrier. The mechanism is based on a monomeric protein, which has all of the functional elements of a transporter; a single central substrate binding site and two networks on either side of the membrane that provide alternating access to the binding site. These features are consistent with the "single binding centre gated pore mechanism" originally proposed by Klingenberg [15, 16], but only if the carriers function as monomers [77]. It is likely that the alternating opening and closing of the carrier requires the simultaneous rotation of the three domains, which is a unique mechanism for transport proteins. Proof of this concept will required the structure of the matrix conformation and the conformational changes to be determined.

Acknowledgements

Our work was funded by the Medical Research Council and the European Community's Seventh Framework Programme FP7/2007-2013 under grant agreement no. HEALTH-F4-2007-201924, EDICT Consortium.

References

[1] F. Palmieri, Mitochondrial transporters of the SLC25 family and associated diseases: a review, Journal of inherited metabolic disease, 37 (2014) 565-575.

[2] H.W. Heldt, H. Jacobs, M. Klingenberg, Endogenous Adp of Mitochondria, an Early Phosphate Acceptor of Oxidative Phosphorylation as Disclosed by Kinetic Studies with C14 Labelled Adp and Atp and with Atractyloside, Biochem. Biophys. Res. Commun., 18 (1965) 174-179.

[3] E. Pfaff, M. Klingenberg, H.W. Heldt, Unspecific permeation and specific exchange of adenine nucleotides in liver mitochondria, Biochim. Biophys. Acta, 104 (1965) 312-315.

[4] E.D. Duee, P.V. Vignais, [Exchange between extra- and intramitochondrial adenine nucleotides], Biochim. Biophys. Acta, 107 (1965) 184-188.

[5] A. Bruni, S. Luciani, Effects of atractyloside and oligomycin on magnesium-stimulated adenosine triphosphatase and on adenosine triphosphate-induced contraction of swollen mitochondria, Nature, 196 (1962) 578-580.

[6] E. Pfaff, M. Klingenberg, Adenine nucleotide translocation of mitochondria. 1. Specificity and control, Eur. J. Biochem., 6 (1968) 66-79.

[7] R. Wulf, A. Kaltstein, M. Klingenberg, H^+ and cation movements associated with ADP, ATP transport in mitochondria, Eur. J. Biochem., 82 (1978) 585-592.

[8] K. LaNoue, S.M. Mizani, M. Klingenberg, Electrical imbalance of adenine nucleotide transport across the mitochondrial membrane, J. Biol. Chem., 253 (1978) 191-198.

[9] M. Klingenberg, H. Rottenberg, Relation between the gradient of the ATP/ADP ratio and the membrane potential across the mitochondrial membrane, Eur. J. Biochem., 73 (1977) 125-130.

[10] P.J. Henderson, H.A. Lardy, Bongkrekic acid. An inhibitor of the adenine nucleotide translocase of mitochondria, J. Biol. Chem., 245 (1970) 1319-1326.

[11] M. Klingenberg, K. Grebe, B. Scherer, Opposite effects of bongkrekic acid and atractyloside on the adenine nucleotides induced mitochondrial volume changes and on the efflux of adenine nucleotides, FEBS Lett.. 16 (1971) 253-256.

[12] P.V. Vignais, P.M. Vignais, G. Defaye, Gummiferin, an inhibitor of the adenine-nucleotide translocation. Study of its binding properties to mitochondria, FEBS Lett., 17 (1971) 281-288.

[13] S. Luciani, N. Martini, R. Santi, Effects of carboxyatractyloside a structural analogue of atractyloside on mitochondrial oxidative phosphorylation, Life Sci II, 10 (1971) 961-968.

[14] G.J. Lauquin, A.M. Duplaa, G. Klein, A. Rousseau, P.V. Vignais, Isobongkrekic acid, a new inhibitor of mitochondrial ADP-ATP transport: radioactive labeling and chemical and biological properties, Biochemistry, 15 (1976) 2323-2327.

[15] H. Erdelt, M.J. Weidemann, M. Buchholz, M. Klingenberg, Some principle effects of bongkrekic acid on the binding of adenine nucleotides to mitochondrial membranes, Eur. J. Biochem., 30 (1972) 107-122.

[16] M. Klingenberg, M. Buchholz, On the mechanism of bongkrekate effect on the mitochondrial adenine-nucleotide carrier as studied through the binding of ADP, Eur. J. Biochem., 38 (1973) 346-358.

[17] O. Jardetzky, Simple Allosteric Model for Membrane Pumps, Nature, 211 (1966) 969 - 970.

[18] P. Riccio, H. Aquila, M. Klingenberg, Purification of the carboxy-atractylate binding protein from mitochondria, FEBS Lett.. 56 (1975) 133-138.

[19] P. Riccio, H. Aquila, M. Klingenberg, Solubilization of the carboxy-atractylate binding protein from mitochondria, FEBS Lett.. 56 (1975) 129-132.

[20] R. Kramer, M. Klingenberg, Reconstitution of adenine nucleotide transport from beef heart mitochondria, Biochemistry, 18 (1979) 4209-4215.

[21] C. Villiers, J.W. Michejda, M. Block, G.J. Lauquin, P.V. Vignais, The electrogenic nature of ADP/ATP transport in inside-out submitochondrial particles, Biochim. Biophys. Acta, 546 (1979) 157-170.

[22] R. Kramer, M. Klingenberg, Electrophoretic control of reconstituted adenine nucleotide translocation, Biochemistry, 21 (1982) 1082-1089.

[23] K. O'Malley, P. Pratt, J. Robertson, M. Lilly, M.G. Douglas, Selection of the nuclear gene for the mitochondrial adenine nucleotide translocator by genetic complementation of the op1 mutation in yeast, J. Biol. Chem., 257 (1982) 2097-2103.

[24] J.E. Lawson, M.G. Douglas, Separate genes encode functionally equivalent ADP/ATP carrier proteins in *Saccharomyces cerevisiae*. Isolation and analysis of AAC2, J. Biol. Chem., 263 (1988) 14812-14818.

[25] J. Kolarov, N. Kolarova, N. Nelson, A third ADP/ATP translocator gene in yeast, J. Biol. Chem., 265 (1990) 12711-12716.

[26] J.E. Lawson, M. Gawaz, M. Klingenberg, M.G. Douglas, Structure-function studies of adenine nucleotide transport in mitochondria. I. Construction and genetic analysis of yeast mutants encoding the ADP/ATP carrier protein of mitochondria, J. Biol. Chem., 265 (1990) 14195-14201.

[27] M. Gawaz, M.G. Douglas, M. Klingenberg, Structure-function studies of adenine nucleotide transport in mitochondria. II. Biochemical analysis of distinct AAC1 and AAC2 proteins in yeast, J. Biol. Chem., 265 (1990) 14202-14208.

[28] W. Visser, A.A. van der Baan, W. Batenburg-van der Vegte, W.A. Scheffers, R. Kramer, J.P. van Dijken, Involvement of mitochondria in the assimilatory metabolism of anaerobic Saccharomyces cerevisiae cultures, Microbiology, 140 (Pt 11) (1994) 3039-3046.

[29] N. Neckelmann, K. Li, R.P. Wade, R. Shuster, D.C. Wallace, cDNA sequence of a human skeletal muscle ADP/ATP translocator: lack of a leader peptide, divergence from a fibroblast translocator cDNA, and coevolution with mitochondrial DNA genes, Proceedings of the National Academy of Sciences of the United States of America, 84 (1987) 7580-7584.

[30] J. Houldsworth, G. Attardi, Two distinct genes for ADP/ATP translocase are expressed at the mRNA level in adult human liver, Proceedings of the National Academy of Sciences of the United States of America, 85 (1988) 377-381.

[31] R. Battini, S. Ferrari, L. Kaczmarek, B. Calabretta, S.T. Chen, R. Baserga, Molecular cloning of a cDNA for a human ADP/ATP carrier which is growth-regulated, The Journal of biological chemistry, 262 (1987) 4355-4359.

[32] R. Slim, J. Levilliers, H.J. Ludecke, U. Claussen, V.C. Nguyen, N.M. Gough, B. Horsthemke, C. Petit, A human pseudoautosomal gene encodes the ANT3 ADP/ATP translocase and escapes X-inactivation, Genomics, 16 (1993) 26-33.

[33] V. Dolce, P. Scarcia, D. Iacopetta, F. Palmieri, A fourth ADP/ATP carrier isoform in man: identification, bacterial expression, functional characterization and tissue distribution, FEBS Lett.. 579 (2005) 633-637.

[34] G. Fiermonte, F. De Leonardis, S. Todisco, L. Palmieri, F.M. Lasorsa, F. Palmieri, Identification of the mitochondrial ATP-Mg/Pi transporter. Bacterial expression,

reconstitution, functional characterization, and tissue distribution, J. Biol. Chem., 279 (2004) 30722-30730.

[35] M.T. Nosek, J.R. Aprille, ATP-Mg/Pi carrier activity in rat liver mitochondria, Arch. Biochem. Biophys., 296 (1992) 691-697.

[36] S.P. Harborne, J.J. Ruprecht, E.R. Kunji, Calcium-induced conformational changes in the regulatory domain of the human mitochondrial ATP-Mg/Pi carrier, Biochimica et biophysica acta, 1847 (2015) 1245-1253.

[37] H. Aquila, D. Misra, M. Eulitz, M. Klingenberg, Complete amino acid sequence of the ADP/ATP carrier from beef heart mitochondria, Hoppe Seylers Z Physiol. Chem., 363 (1982) 345-349.

[38] M. Saraste, J.E. Walker, Internal sequence repeats and the path of polypeptide in mitochondrial ADP/ATP translocase, FEBS Lett.. 144 (1982) 250-254.

[39] H. Aquila, T.A. Link, M. Klingenberg, The uncoupling protein from brown fat mitochondria is related to the mitochondrial ADP/ATP carrier., EMBO J., 4 (1985) 2369-2376.

[40] M.J. Runswick, S.J. Powell, P. Nyren, J.E. Walker, Sequence of the bovine mitochondrial phosphate carrier protein: structural relationship to ADP/ATP translocase and the brown fat mitochondria uncoupling protein, EMBO J., 6 (1987) 1367-1373.

[41] S.J. Powell, S.M. Medd, M.J. Runswick, J.E. Walker, Two bovine genes for mitochondrial ADP/ATP translocase expressed differences in various tissues, Biochemistry, 28 (1989) 866-873.

[42] M.J. Runswick, J.E. Walker, F. Bisaccia, V. Iacobazzi, F. Palmieri, Sequence of the bovine 2-oxoglutarate/malate carrier protein: structural relationship to other mitochondrial transport proteins, Biochemistry, 29 (1990) 11033-11040.

[43] D.R. Nelson, C.M. Felix, J.M. Swanson, Highly conserved charge-pair networks in the mitochondrial carrier family, J. Mol. Biol., 277 (1998) 285-308.

[44] J.E. Walker, The mitochondrial transporter family, Current opinion in structural biology, 2 (1992) 519-526.

[45] B. Miroux, V. Frossard, S. Raimbault, D. Ricquier, F. Bouillaud, The topology of the brown adipose tissue mitochondrial uncoupling protein determined with antibodies against its antigenic sites revealed by a library of fusion proteins, The EMBO journal, 12 (1993) 3739-3745.

[46] L. Capobianco, F. Bisaccia, A. Michel, F.E. Sluse, F. Palmieri, The N- and C-termini of the tricarboxylate carrier are exposed to the cytoplasmic side of the inner mitochondrial membrane, FEBS Lett.. 357 (1995) 297-300.

[47] G. Brandolin, F. Boulay, P. Dalbon, P.V. Vignais, Orientation of the N-terminal region of the membrane-bound ADP/ATP carrier protein explored by antipeptide antibodies and an arginine-specific endoprotease. Evidence that the accessibility of the N-terminal residues depends on the conformational state of the carrier, Biochemistry, 28 (1989) 1093-1100.

[48] C. Eckerskorn, M. Klingenberg, In the uncoupling protein from brown adipose tissue the C-terminus protrudes to the c-side of the membrane as shown by tryptic cleavage, FEBS Lett.. 226 (1987) 166-170.

[49] E.R.S. Kunji, M. Harding, Projection structure of the atractyloside-inhibited mitochondrial ADP/ATP carrier of *Saccharomyces cerevisiae*, J. Biol. Chem., 278 (2003) 36985-36988.

[50] E.R.S. Kunji, The role and structure of mitochondrial carriers, FEBS Lett., 564 (2004) 239-244.

[51] H. Aquila, W. Eiermann, W. Babel, M. Klingenberg, Isolation of the ADP/ATP translocator from beef heart mitochondria as the bongkrekate-protein complex, Eur. J. Biochem., 85 (1978) 549-560.

[52] M.R. Block, G. Zaccai, G.J. Lauquin, P.V. Vignais, Small angle neutron scattering of the mitochondrial ADP/ATP carrier protein in detergent, Biochem. Biophys. Res. Commun., 109 (1982) 471-477.

[53] G. Brandolin, J. Doussiere, A. Gulik, T. Gulik-Krzywicki, G.J. Lauquin, P.V. Vignais, Kinetic, binding and ultrastructural properties of the beef heart adenine nucleotide carrier protein after incorporation into phospholipid vesicles, Biochim. Biophys. Acta, 592 (1980) 592-614.

[54] H. Hackenberg, M. Klingenberg, Molecular weight and hydrodynamic parameters of the adenosine 5'-diphosphate--adenosine 5'-triphosphate carrier in Triton X-100, Biochemistry, 19 (1980) 548-555.

[55] M.T. Ryan, H. Muller, N. Pfanner, Functional staging of ADP/ATP carrier translocation across the outer mitochondrial membrane, J. Biol. Chem., 274 (1999) 20619-20627.

[56] K.N. Truscott, N. Wiedemann, P. Rehling, H. Muller, C. Meisinger, N. Pfanner, B. Guiard, Mitochondrial import of the ADP/ATP carrier: the essential TIM complex of

the intermembrane space is required for precursor release from the TOM complex, Mol. Cell Biol., 22 (2002) 7780-7789.

[57] F. Jiang, M.T. Ryan, M. Schlame, M. Zhao, Z. Gu, M. Klingenberg, N. Pfanner, M.L. Greenberg, Absence of cardiolipin in the crd1 null mutant results in decreased mitochondrial membrane potential and reduced mitochondrial function, J. Biol. Chem., 275 (2000) 22387-22394.

[58] S.D. Dyall, S.C. Agius, C. De Marcos Lousa, V. Trezeguet, K. Tokatlidis, The dynamic dimerization of the yeast ADP/ATP carrier in the inner mitochondrial membrane is affected by conserved cysteine residues, J. Biol. Chem., 278 (2003) 26757-26764.

[59] E. Majima, K. Ikawa, M. Takeda, M. Hashimoto, Y. Shinohara, H. Terada, Translocation of loops regulates transport activity of mitochondrial ADP/ATP carrier deduced from formation of a specific intermolecular disulfide bridge catalyzed by copper-o-phenanthroline, J. Biol. Chem., 270 (1995) 29548-29554.

[60] M. Hashimoto, E. Majima, S. Goto, Y. Shinohara, H. Terada, Fluctuation of the first loop facing the matrix of the mitochondrial ADP/ATP carrier deduced from intermolecular cross-linking of Cys56 residues by bifunctional dimaleimides, Biochemistry, 38 (1999) 1050-1056.

[61] E. Majima, M. Takeda, S. Miki, Y. Shinohara, H. Terada, Close location of the first loop to the third loop of the mitochondrial ADP/ATP carrier deduced from cross-linking catalyzed by copper-o-phenanthroline of the solubilized carrier with Triton X-100, J. Biochem., 131 (2002) 461-468.

[62] S.G. Huang, S. Odoy, M. Klingenberg, Chimers of two fused ADP/ATP carrier monomers indicate a single channel for ADP/ATP transport, Arch. Biochem. Biophys., 394 (2001) 67-75.

[63] V. Postis, C. De Marcos Lousa, B. Arnou, G.J. Lauquin, V. Trezeguet, Subunits of the Yeast Mitochondrial ADP/ATP Carrier: Cooperation within the Dimer, Biochemistry, 44 (2005) 14732-14740.

[64] T. Gropp, N. Brustovetsky, M. Klingenberg, V. Muller, K. Fendler, E. Bamberg, Kinetics of electrogenic transport by the ADP/ATP carrier, Biophys. J., 77 (1999) 714-726.

[65] R. Krämer, F. Palmieri, Metabolite carriers in mitochondria, in: L. Ernster (Ed.) Molecular mechanism in Bioenergetics, Elsevier Science Publisher B.V., Amsterdam, 1992, pp. 359-384.

[66] C. Duyckaerts, C.M. Sluse-Goffart, J.P. Fux, F.E. Sluse, C. Liebecq, Kinetic mechanism of the exchanges catalysed by the adenine-nucleotide carrier, Eur. J. Biochem., 106 (1980) 1-6.

[67] J.J. Ruprecht, A.M. Hellawell, M. Harding, P.G. Crichton, A.J. Mccoy, E.R.S. Kunji, Structures of yeast mitochondrial ADP/ATP carriers support a domain-based alternating-access transport mechanism, Proc. Natl. Acad. Sci. U.S.A, 111 (2014) E426-E434.

[68] E. Pebay-Peyroula, C. Dahout-Gonzalez, R. Kahn, V. Trezeguet, G.J. Lauquin, G. Brandolin, Structure of mitochondrial ADP/ATP carrier in complex with carboxyatractyloside, Nature, 426 (2003) 39-44.

[69] H. Nury, C. Dahout-Gonzalez, V. Trezeguet, G. Lauquin, G. Brandolin, E. Pebay-Peyroula, Structural basis for lipid-mediated interactions between mitochondrial ADP/ATP carrier monomers, FEBS Lett.. 579 (2005) 6031-6036.

[70] L. Bamber, M. Harding, P.J.G. Butler, E.R.S. Kunji, Yeast mitochondrial ADP/ATP carriers are monomeric in detergents, Proc. Natl. Acad. Sci. U.S.A., 103 (2006) 16224-16229.

[71] L. Bamber, D.J. Slotboom, E.R.S. Kunji, Yeast mitochondrial ADP/ATP carriers are monomeric in detergents as demonstrated by differential affinity purification, J. Mol. Biol., 371 (2007) 388-395.

[72] P.G. Crichton, E.R.S. Kunji, Determining the oligomeric state of mitochondrial carrier proteins by blue native gel electrophoresis, Bba-Bioenergetics, 1797 (2010) 43-43.

[73] H. Nury, F. Manon, B. Arnou, M. le Maire, E. Pebay-Peyroula, C. Ebel, Mitochondrial bovine ADP/ATP carrier in detergent is predominantly monomeric, but also forms multimeric species, Biochemistry, 43 (2008) 12319-12331.

[74] A. Kedrov, A.M. Hellawell, A. Klosin, R.B. Broadhurst, E.R.S. Kunji, D.J. Muller, Probing the interactions of carboxy-atractyloside and atractyloside with the yeast mitochondrial ADP/ATP Carrier, Structure, 18 (2010) 39-46.

[75] L. Bamber, M. Harding, M. Monné, D.J. Slotboom, E.R.S. Kunji, The yeast mitochondrial ADP/ATP carrier functions as a monomer in mitochondrial membranes, Proc. Natl. Acad. Sci. U.S.A., 104 (2007) 10830-10834.

[76] P.G. Crichton, M. Harding, J.J. Ruprecht, Y. Lee, E.R.S. Kunji, Lipid, detergent, and Coomassie Blue G-250 affect the migration of small membrane proteins in blue

native gels; mitochondrial carriers migrate as monomers not dimers, J. Biol. Chem., 288 (2013) 22163-22173.

[77] E.R.S. Kunji, P.G. Crichton, Mitochondrial carriers function as monomers, Biochim. Biophys. Acta, 1797 (2010) 817-831.

[78] Y. Lee, C. Willers, E.R. Kunji, P.G. Crichton, Uncoupling protein 1 binds one nucleotide per monomer and is stabilized by tightly bound cardiolipin, Proceedings of the National Academy of Sciences of the United States of America, 112 (2015) 6973-6978.

[79] C. Thangaratnarajah, J.J. Ruprecht, E.R. Kunji, Calcium-induced conformational changes of the regulatory domain of human mitochondrial aspartate/glutamate carriers, Nature communications, 5 (2014) 5491.

[80] J.F. Sanchez, B. Kauffmann, A. Grelard, C. Sanchez, V. Trezeguet, I. Huc, G.J. Lauquin, Unambiguous structure of atractyloside and carboxyatractyloside, Bioorg. Med. Chem. Lett., 22 (2012) 2973-2975.

[81] A. Hellawell, A. Kedrov, A. Klosin, R.B. Broadhurst, E.R.S. Kunji, D. Muller, Effects of inhibitors on the unfolding of the mitochondrial ADP/ATP carrier by single-molecule force spectroscopy, Bba-Bioenergetics, 1777 (2008) 26-26.

[82] K. Beyer, M. Klingenberg, ADP/ATP carrier protein from beef heart mitochondria has high amounts of tightly bound cardiolipin, as revealed by 31P nuclear magnetic resonance, Biochemistry, 24 (1985) 3821-3826.

[83] F. Jiang, H.S. Rizavi, M.L. Greenberg, Cardiolipin is not essential for the growth of *Saccharomyces cerevisiae* on fermentable or non-fermentable carbon sources, Mol. Microbiol., 26 (1997) 481-491.

[84] A. Haghighi, T.B. Haack, M. Atiq, H. Mottaghi, H. Haghighi-Kakhki, R.A. Bashir, U. Ahting, R.G. Feichtinger, J.A. Mayr, A. Rotig, A.S. Lebre, T. Klopstock, A. Dworschak, N. Pulido, M.A. Saeed, N. Saleh-Gohari, E. Holzerova, P.F. Chinnery, R.W. Taylor, H. Prokisch, Sengers syndrome: six novel AGK mutations in seven new families and review of the phenotypic and mutational spectrum of 29 patients, Orphanet journal of rare diseases, 9 (2014) 119.

[85] J.A. Mayr, T.B. Haack, E. Graf, F.A. Zimmermann, T. Wieland, B. Haberberger, A. Superti-Furga, J. Kirschner, B. Steinmann, M.R. Baumgartner, I. Moroni, E. Lamantea, M. Zeviani, R.J. Rodenburg, J. Smeitink, T.M. Strom, T. Meitinger, W. Sperl, H. Prokisch, Lack of the mitochondrial protein acylglycerol kinase causes Sengers syndrome, Am J Hum Genet, 90 (2012) 314-320.

[86] G. Olofsson, E. Sparr, Ionization Constants pKa of Cardiolipin, PloS one, 8 (2013) e73040.

[87] F. Dehez, E. Pebay-Peyroula, C. Chipot, Binding of ADP in the mitochondrial ADP/ATP carrier is driven by an electrostatic funnel, J. Am. Chem. Soc., 130 (2008) 12725-12733.

[88] E.M. Krammer, S. Ravaud, F. Dehez, A. Frelet-Barrand, E. Pebay-Peyroula, C. Chipot, High-chloride concentrations abolish the binding of adenine nucleotides in the mitochondrial ADP/ATP carrier family, Biophys J, 97 (2009) L25-27.

[89] J. Mifsud, S. Ravaud, E.M. Krammer, C. Chipot, E.R.S. Kunji, E. Pebay-Peyroula, F. Dehez, The substrate specificity of the human ADP/ATP carrier AAC1, Mol. Membr. Biol., 30 (2013) 160-168.

[90] A.J. Robinson, E.R.S. Kunji, Mitochondrial carriers in the cytoplasmic state have a common substrate binding site, Proc. Natl. Acad. Sci. U.S.A., 103 (2006) 2617-2622.

[91] E.R.S. Kunji, A.J. Robinson, The conserved substrate binding site of mitochondrial carriers, Biochimica Biophysica Acta, 1757 (2006) 1237-1248.

[92] A.J. Robinson, C. Overy, E.R.S. Kunji, The mechanism of transport by mitochondrial carriers based on analysis of symmetry, Proc. Natl. Acad. Sci. U.S.A., 105 (2008) 17766-17771.

[93] Y. Wang, E. Tajkhorshid, Electrostatic funneling of substrate in mitochondrial inner membrane carriers, Proc. Natl. Acad. Sci. U.S.A., 105 (2008) 9598-9603.

[94] P. Dalbon, G. Brandolin, F. Boulay, J. Hoppe, P.V. Vignais, Mapping of the nucleotide-binding sites in the ADP/ATP carrier of beef heart mitochondria by photolabeling with 2-azido[alpha-32P]adenosine diphosphate, Biochemistry, 27 (1988) 5141-5149.

[95] C. David, B. Arnou, J.F. Sanchez, L. Pelosi, G. Brandolin, G.J. Lauquin, V. Trezeguet, Two Residues of a Conserved Aromatic Ladder of the Mitochondrial ADP/ATP Carrier Are Crucial to Nucleotide Transport (dagger), Biochemistry, (2008).

[96] M.S. King, M. Kerr, P.G. Crichton, R. Springett, E.R. Kunji, Formation of a cytoplasmic salt bridge network in the matrix state is a fundamental step in the transport mechanism of the mitochondrial ADP/ATP carrier, Biochimica et biophysica acta, 1857 (2016) 14-22.

[97] A.I. Alexandrov, M. Mileni, E.Y. Chien, M.A. Hanson, R.C. Stevens, Microscale fluorescent thermal stability assay for membrane proteins, Structure, 16 (2008) 351-359.

[98] P.G. Crichton, Y. Lee, J.J. Ruprecht, E. Cerson, C. Thangaratnarajah, M.S. King, E.R.S. Kunji, Trends in thermostability provide information on the nature of

substrate, inhibitor, and lipid interactions with mitochondrial carriers, J. Biol. Chem., 290 (2015) 8206-8217.

[99] A.R. Cappello, D.V. Miniero, R. Curcio, A. Ludovico, L. Daddabbo, I. Stipani, A.J. Robinson, E.R. Kunji, F. Palmieri, Functional and structural role of amino acid residues in the odd-numbered transmembrane alpha-helices of the bovine mitochondrial oxoglutarate carrier, J. Mol. Biol., 369 (2007) 400-412.

[100] W.P. Russ, D.M. Engelman, The GxxxG motif: a framework for transmembrane helix-helix association, J. Mol. Biol., 296 (2000) 911-919.

[101] A. Zhou, A. Rohou, D.G. Schep, J.V. Bason, M.G. Montgomery, J.E. Walker, N. Grigorieff, J.L. Rubinstein, Structure and conformational states of the bovine mitochondrial ATP synthase by cryo-EM, eLife, 4 (2015).

[102] I.N. Watt, M.G. Montgomery, M.J. Runswick, A.G. Leslie, J.E. Walker, Bioenergetic cost of making an adenosine triphosphate molecule in animal mitochondria, Proceedings of the National Academy of Sciences of the United States of America, 107 (2010) 16823-16827.

Legends to the figures

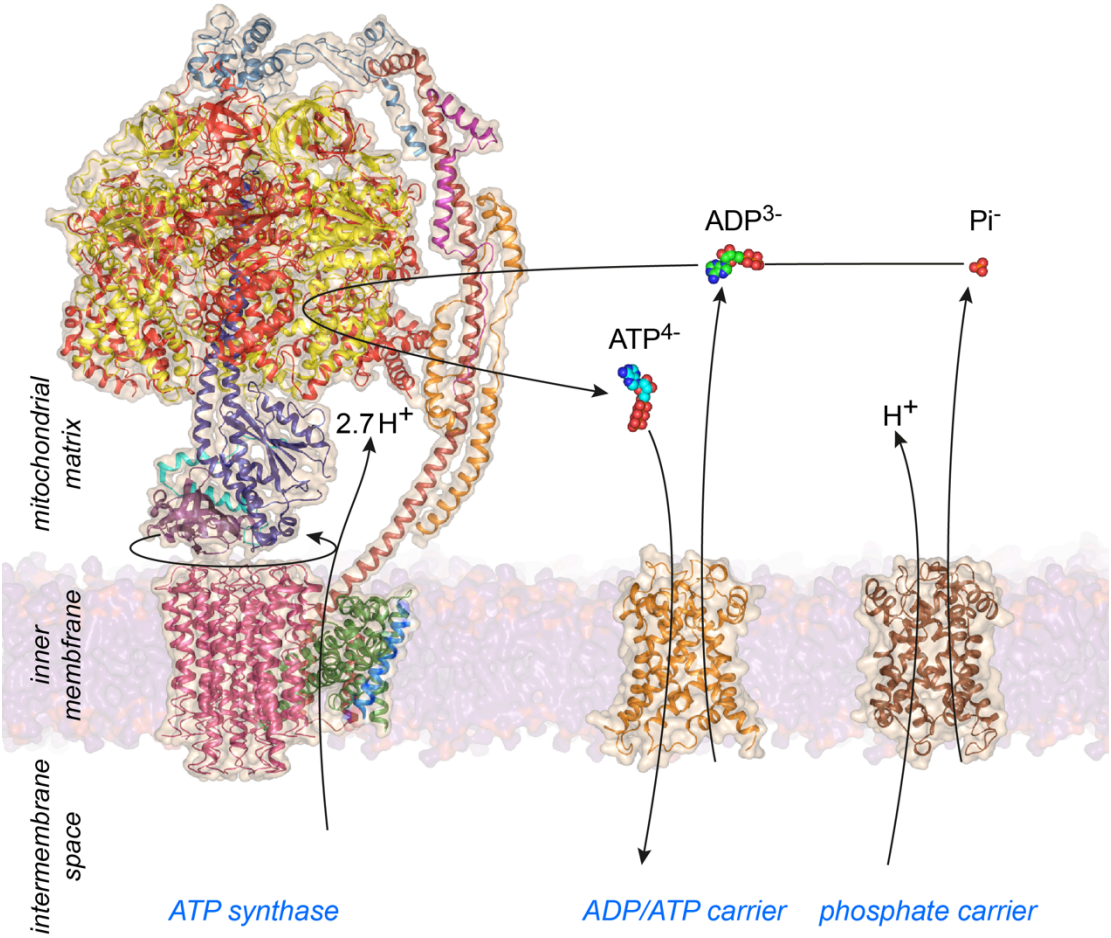

Figure 1. Mitochondrial ADP/ATP and phosphate carriers and ATP synthase. The mitochondrial ADP/ATP carrier and phosphate carrier are shown in orange and brown, respectively. ATP synthase is shown as a poly-alanine model based on single particle analysis [101]. The complex consists of catalytic subunits α (red) and β (yellow); central stalk subunits c (magenta), d (purple), e (light blue), and g (dark blue); peripheral stalk subunits OSCP (blue), F6 (violet), b (dark red) and d (orange); proton-translocating subunit a (green); subunit A6L (marine). Eight proton translocation steps are required to make three ATP molecules, or 2.7 H^+ per ATP [102]. Key transport steps are indicated by arrows.

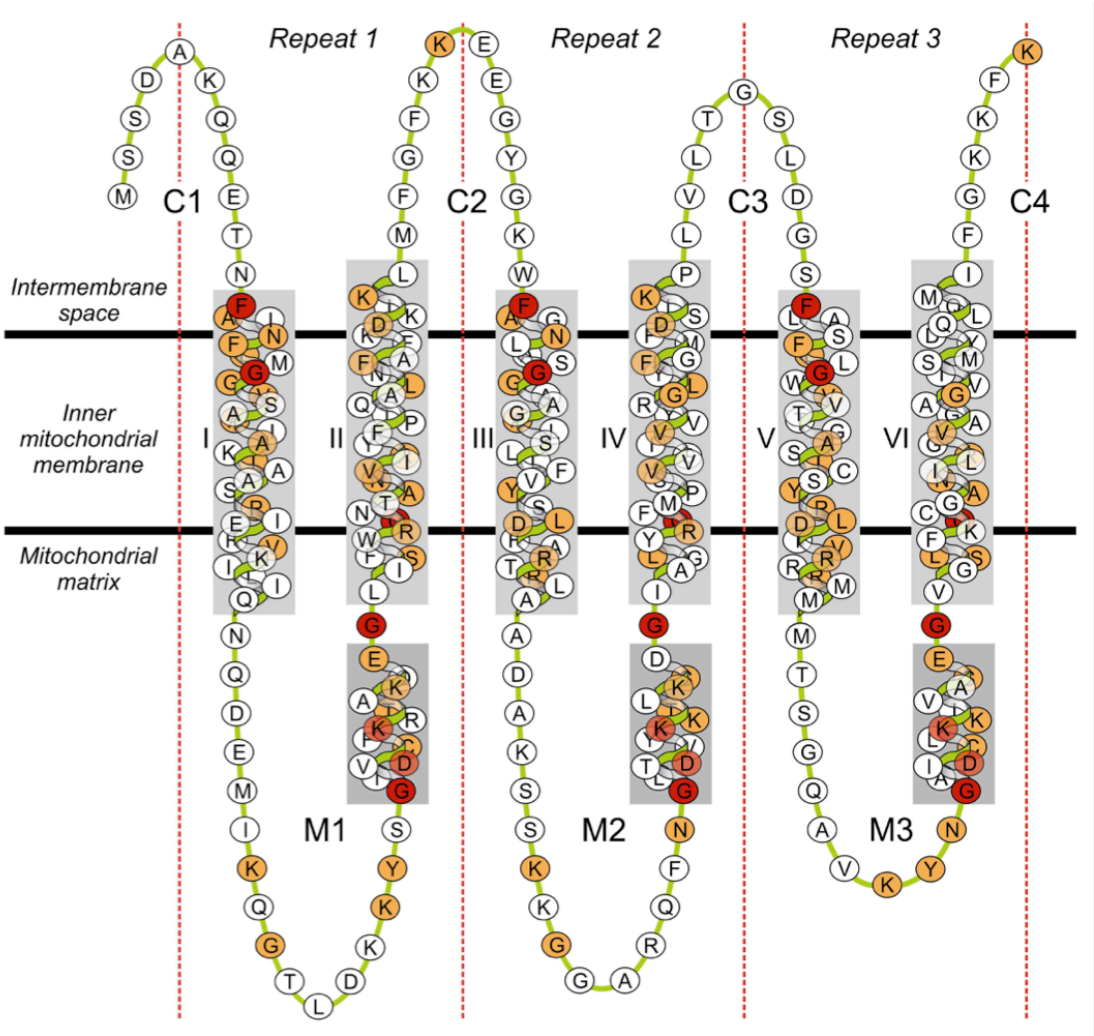

Figure 2 Topology model of the yeast ADP/ATP carrier Aac3p. Red dotted lines indicate the borders of the three sequence repeats of the tripartite structure. The red residues are conserved in all three repeats, whereas the orange residues are conserved in two out of three repeats. The loops in the mitochondrial matrix are named M1, M2 and M3, whereas the termini and cytoplasmic loops are named C1, C2, C3 and C4. The helices are indicated with Roman numerals on the left hand side of the helices.

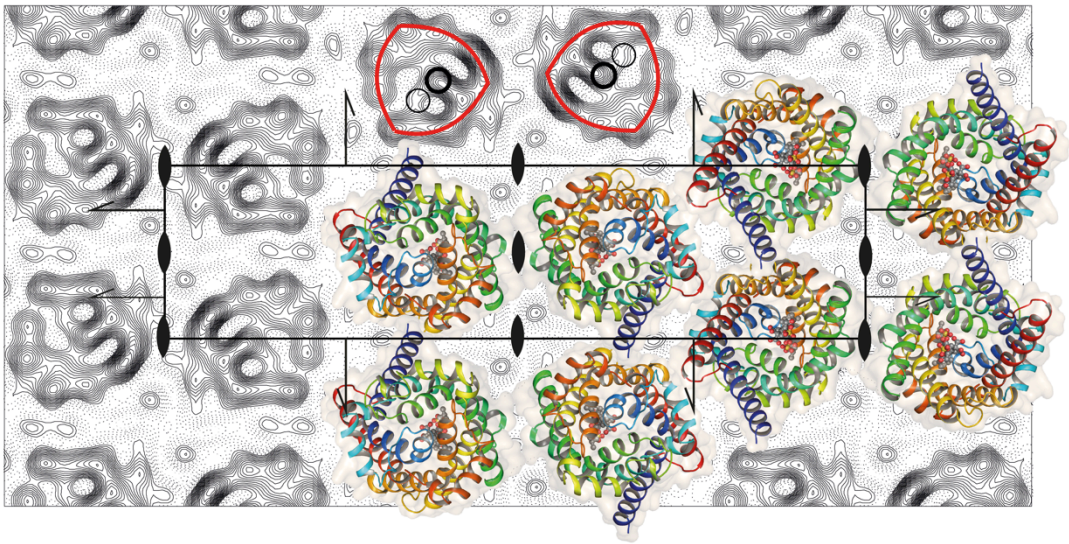

Figure 3 Projection structure of the yeast mitochondrial ADP/ATP carrier Aac3p by electron crystallography. Projection electron density map of Aac3p at 5-Å resolution calculated from merged amplitudes and phases from two independent crystal lattices with $p22_12_1$ symmetry imposed [49]. A unit cell is displayed with the a-axis (42.5 Å) vertical and the b-axis (172.1 Å) horizontal. Also shown are the 2-fold axes perpendicular to the membrane and the screw axes in the plane of the membrane. Solid lines indicate density above the mean, while negative contours are shown as dotted lines. The rounded triangles (shown in red) emphasise the three-fold pseudo-symmetry of Aac3p. The strong and weak asymmetrical densities are indicated by bold and light black circles, respectively. Because of the crystal symmetry there are rows of crystallographic dimers of yeast Aac3p [67], oriented up and down alternatingly. The Aac3p structural models are shown in cartoon representation and rainbow colour scheme from the N-terminus in blue to the C-terminus in red. CATR is shown in a ball and stick presentation.

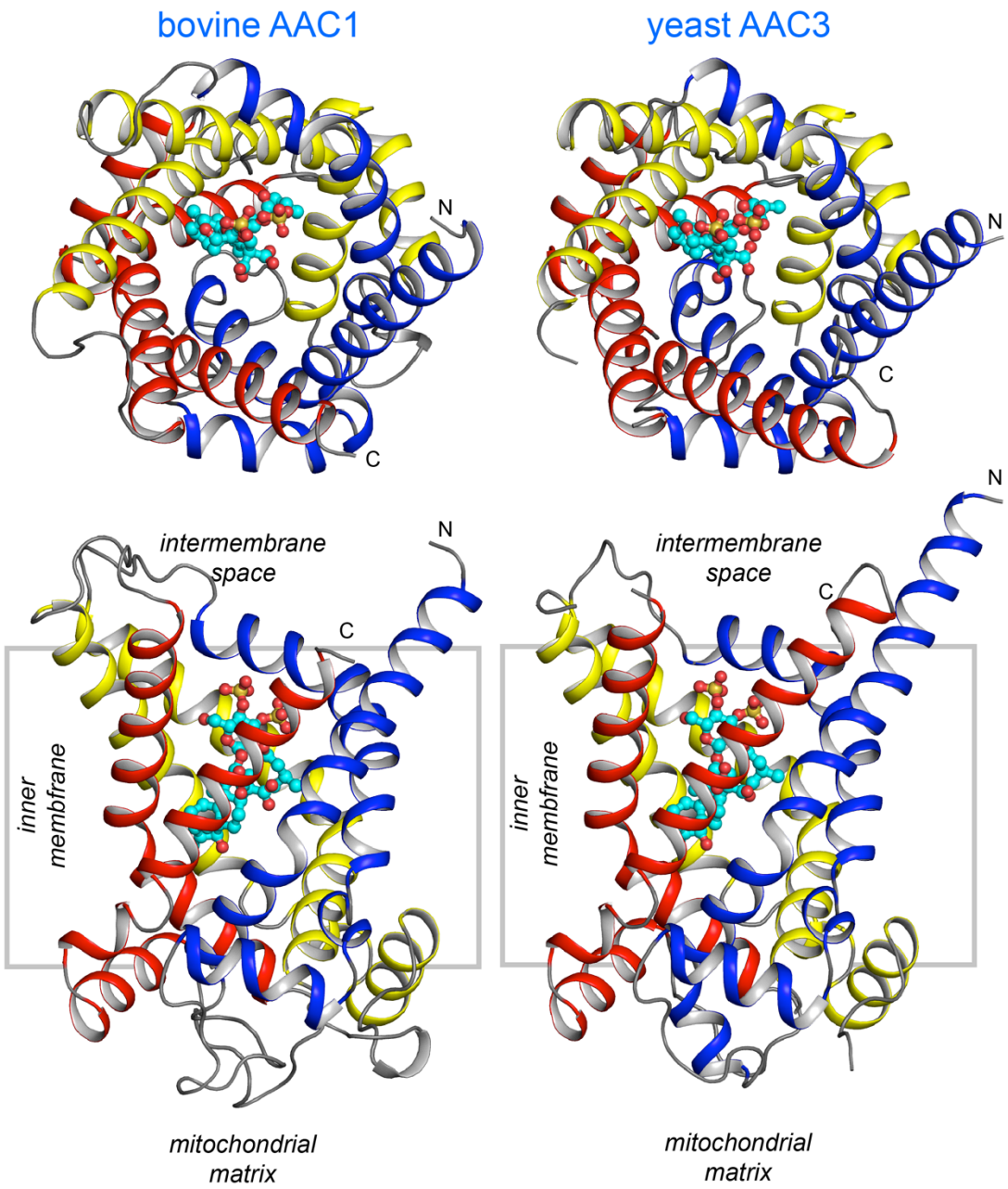

Figure 4 Architecture of the bovine and yeast ADP/ATP carrier by x-ray crystallography. Structures of the bovine ADP/ATP carrier AAC1 (1OKC) [68] (left) and the yeast ADP/ATP carrier Aac3p (4C9Q) [67] (right). Repeats 1, 2 and 3 are shown in blue, yellow and red cartoon representation, respectively. Residues 1 and 294-297 are missing in the structure of AAC1, whereas residues 1-2, 149-155, and 208-214 are missing in the structure of Aac3p, as these protein regions are highly mobile. Also shown is CATR in cyan ball and stick representation.

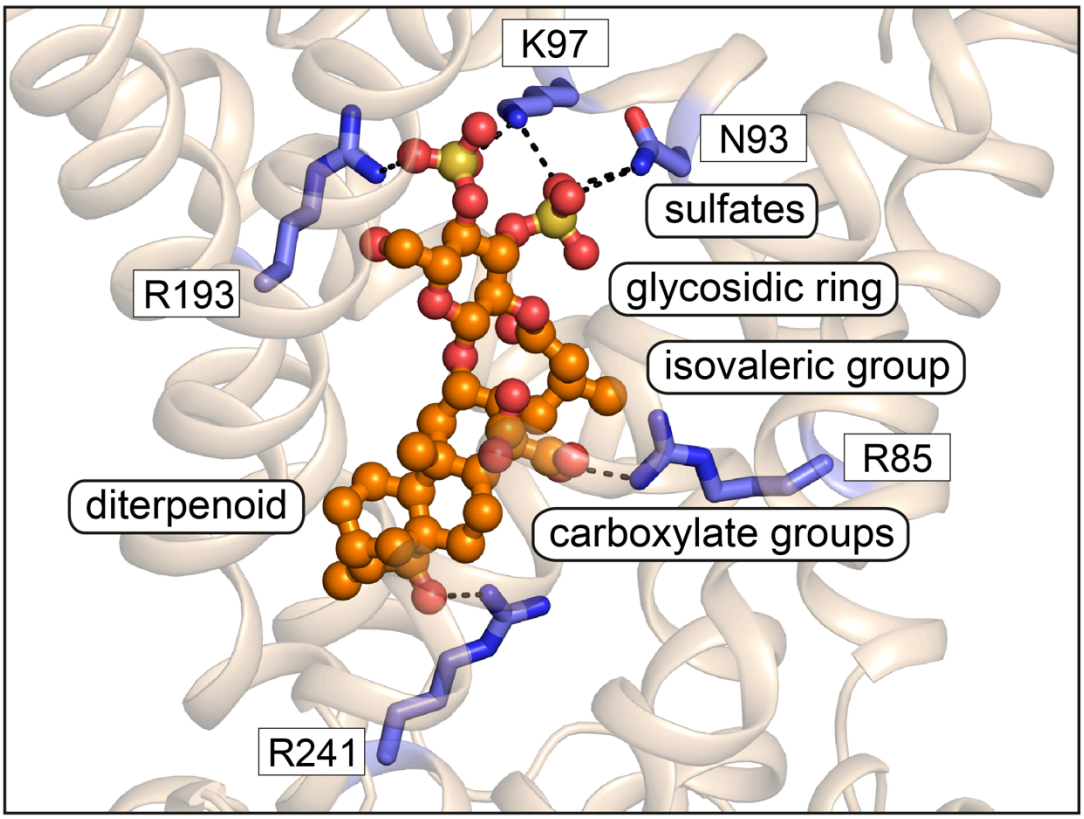

Figure 5 Carboxyatractyloside binding to the yeast mitochondrial ADP/ATP carrier Aac3p. CATR is shown in stick and sphere representation bound to Aac3p (4C9Q) [67] and is modelled with a β-D-glucoside ring [80]. The functional moieties of CATR are also indicated. Residues interacting with the inhibitor are shown in blue stick representations and are labelled accordingly. Polar interactions between CATR and residues are shown as black dashed lines.

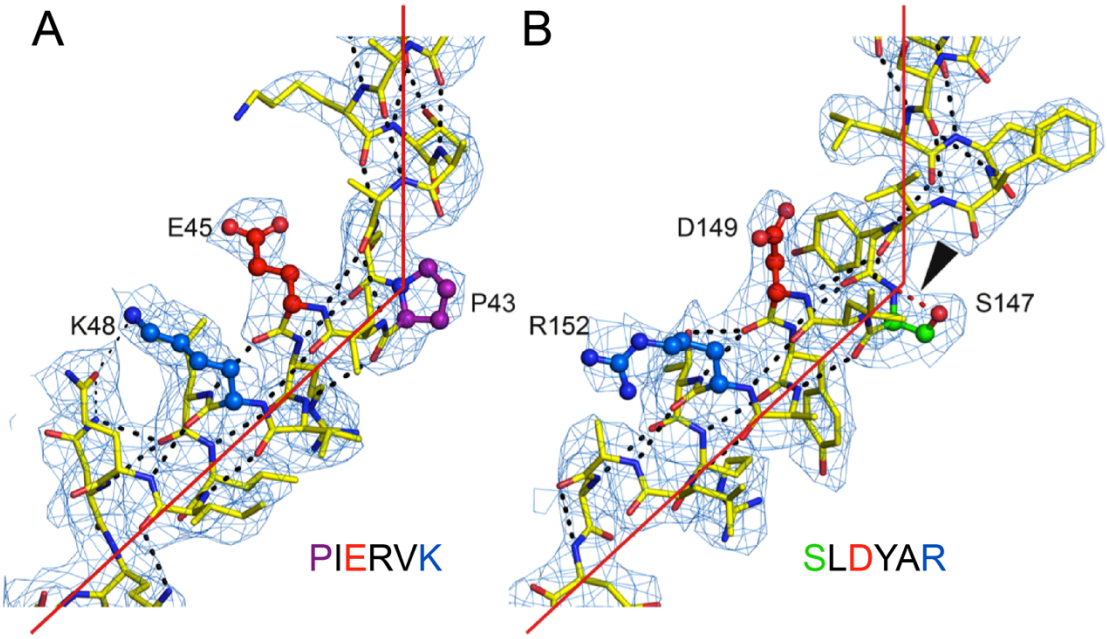

Figure 6 Proline and serine residues in the signature motifs of Aac2p. (A) The signature motif of H1 and (B) of H3. Residues interacting with the side-chains are shown in line representation. The positively charged, negative charged, polar and proline residues of the signature motif (sequence shown below) are in blue, red, green and purple, respectively. Hydrogen bonds involving backbone atoms are shown as thick black dotted lines, hydrogen bonds not involving backbone atoms are shown as thin black dotted lines. The density, shown as a blue mesh, is a 2mFo-DFc map, contoured at 1 σ, and displayed within 2 Å of the atoms. In (B), the unusual hydrogen bond from the side-chain of Ser147 to its own backbone amide is highlighted in red dots, and indicated by an arrowhead.

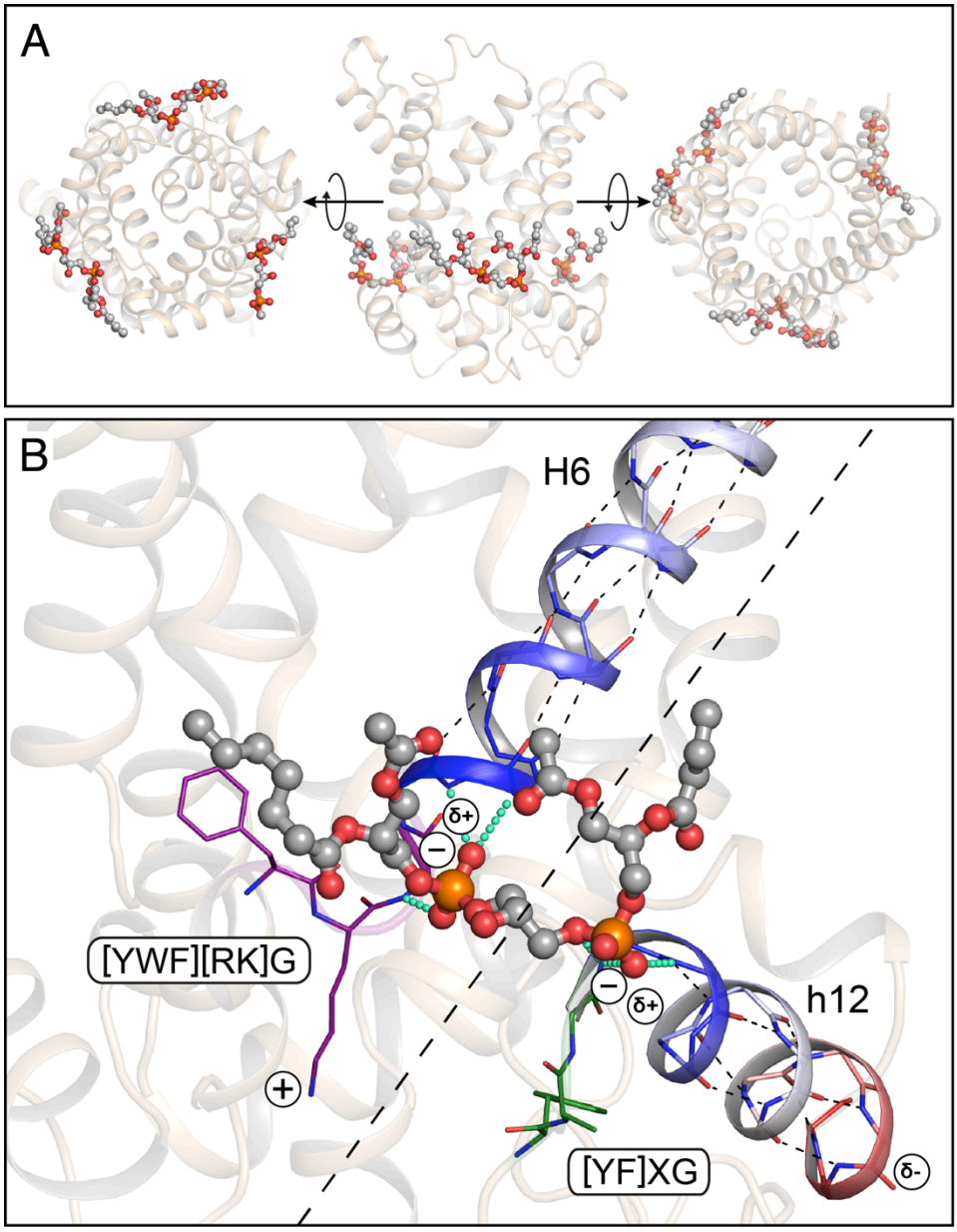

Figure 7 Cardiolipin binding site of the yeast ADP/ATP carrier. (A) Different views of the three cardiolipin-binding sites of Aac2p [67]. The protein and cardiolipin molecules are shown in wheat cartoon and CPK ball-and-stick representations, respectively. The cardiolipin acyl chains have only been partially modelled. (B) Detailed view of the binding site for cardiolipin. The carrier is shown in wheat cartoon representation. Hydrogen bonds within the helices are shown as thin black dotted lines. Residues in the [YWF][KR]G and [YF]XG motifs are shown in violet and green, respectively. Hydrogen bond interactions between protein and cardiolipin are shown as thick cyan dashed lines.

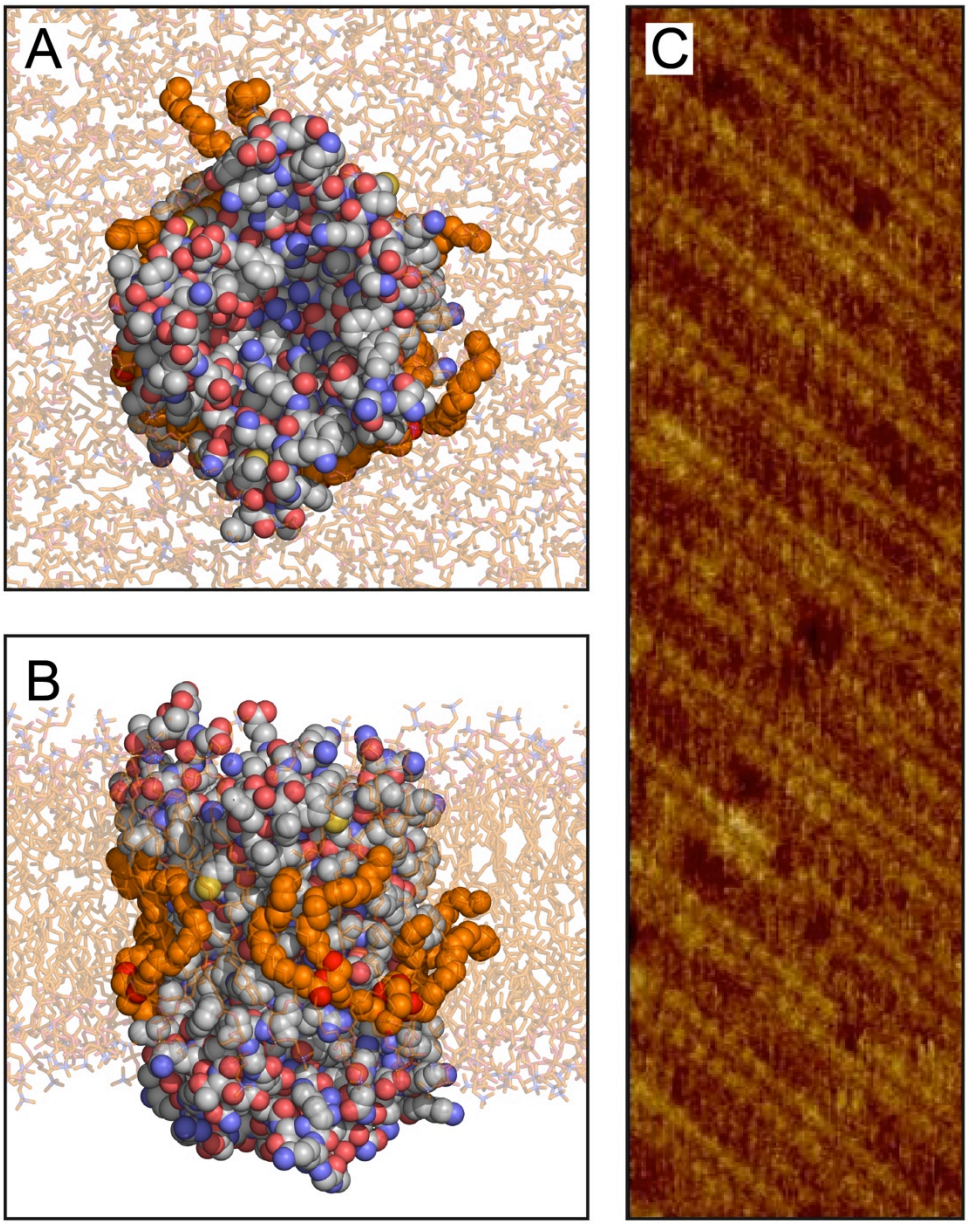

Figure 8 Yeast ADP/ATP carriers in the membrane – molecular dynamics simulations and atomic force microscopy. A Cytoplasmic and B lateral view of Aac2p in a dioleoylphosphatidylcholine bilayer (orange stick representation). Aac2p and cardiolipin molecules are shown in CPK and orange sphere representations, respectively. Aac2p [67] and cardiolipin molecules complete with oleoyl chains were equilibrated and simulated for 2 ns. C High-resolution atomic force microscopy topograph of a two dimensional crystal (similar to Figure 2). Because of the crystal symmetry, the crystal in a dioleoyl phosphocholine bilayer contains rows of Aac3p crystallographic dimers with matrix side up or down orientations [74].

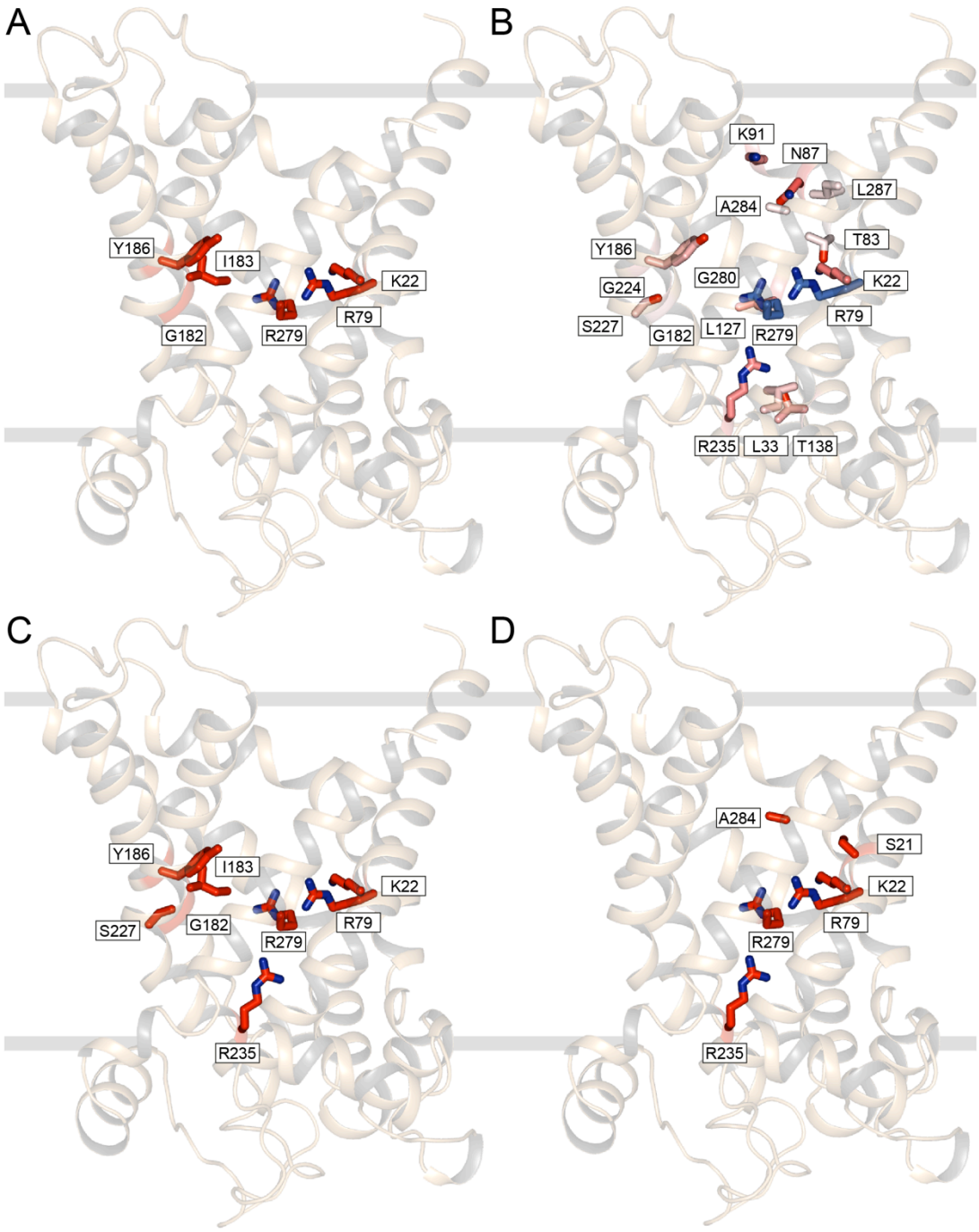

Figure 9 Different approaches used for identification of the substrate binding site. The substrate binding site of AAC1 identified by (A) chemical and distance constraints [90, 91], by (B) symmetry analysis [92], and by (C) and (D) molecular dynamics simulations [87, 89, 93]. The key residues are shown as red sticks, except for (B), where the sticks are coloured according to their symmetry score from highly asymmetric (red) to neutral (white) to highly symmetric (blue).

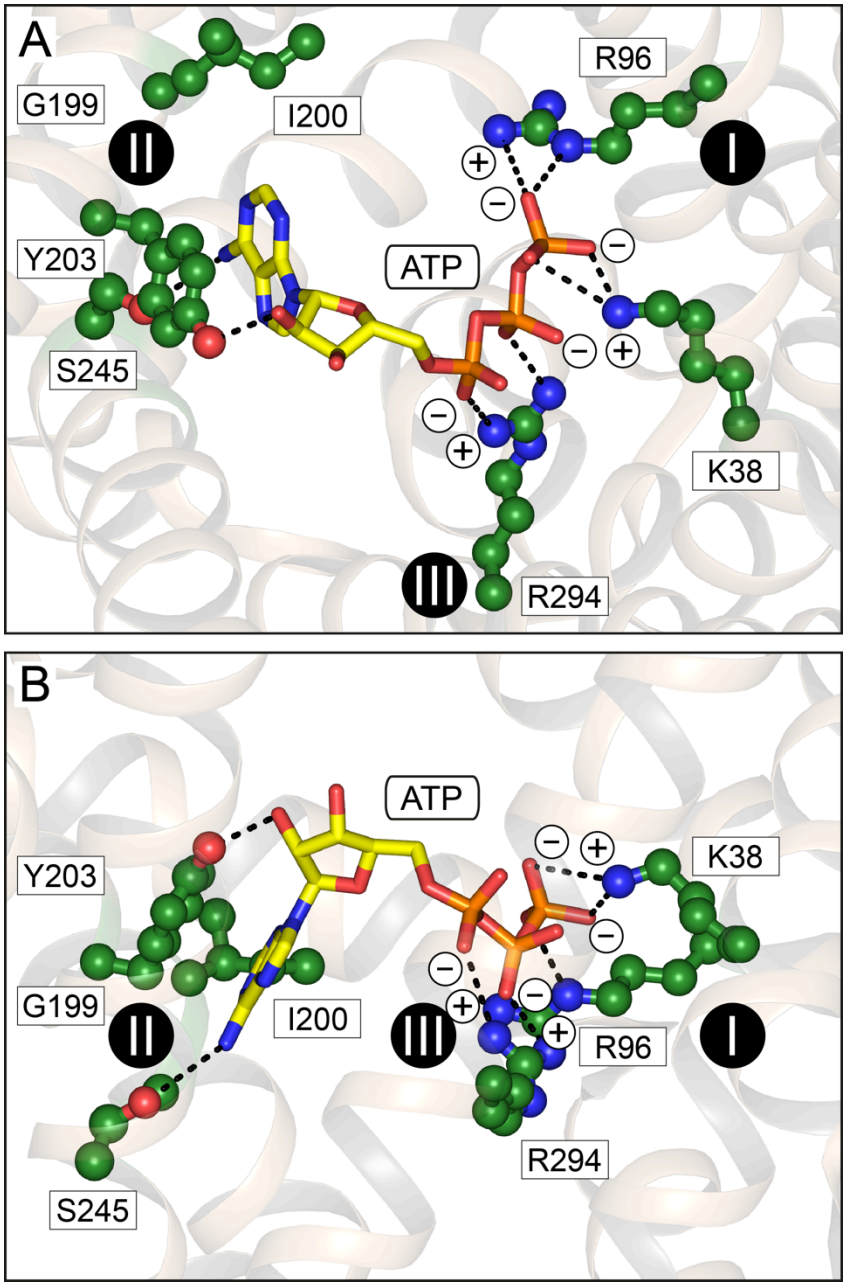

Figure 10 Putative substrate binding site of the mitochondrial ADP/ATP carrier. Proposed pose of ATP on the substrate binding site of the yeast ADP/ATP carrier Aac2p [67], shown (A) above from the intermembrane space and (B) laterally from the membrane. The ATP is shown in yellow stick representation, whereas the residues of the binding site are shown in green ball-and-stick representation. Indicated by roman numerals are the contact points of the binding site [90, 91]. ATP has four negative charges, whereas the substrate binding site has three positively charged residues, leaving a net charge of minus one.

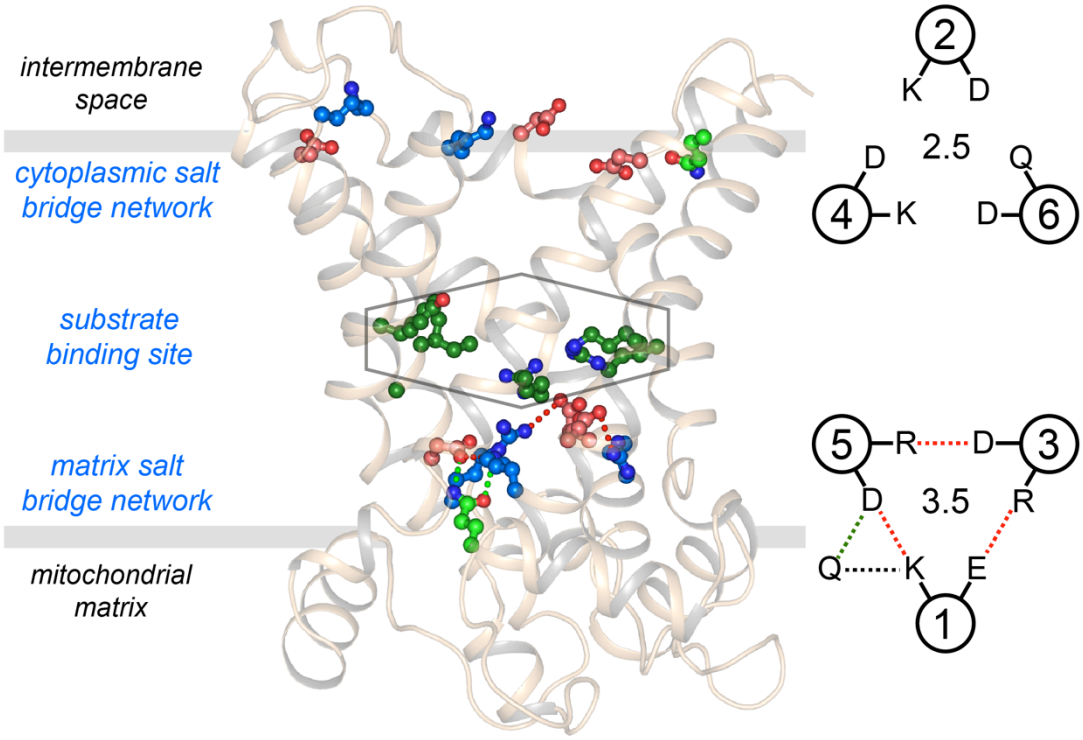

Figure 11 Main functional elements of the mitochondrial ADP/ATP carrier. Lateral view of the yeast Aac2p [67] in cartoon representation, showing the central substrate binding site (stick), the cytoplasmic salt bridge network (top, ball and stick), and the matrix salt bridge network (bottom, ball and stick). Positively charged, negatively charged and polar residues are shown in blue, red, and green, respectively. Also shown are the two networks in schematic representations.

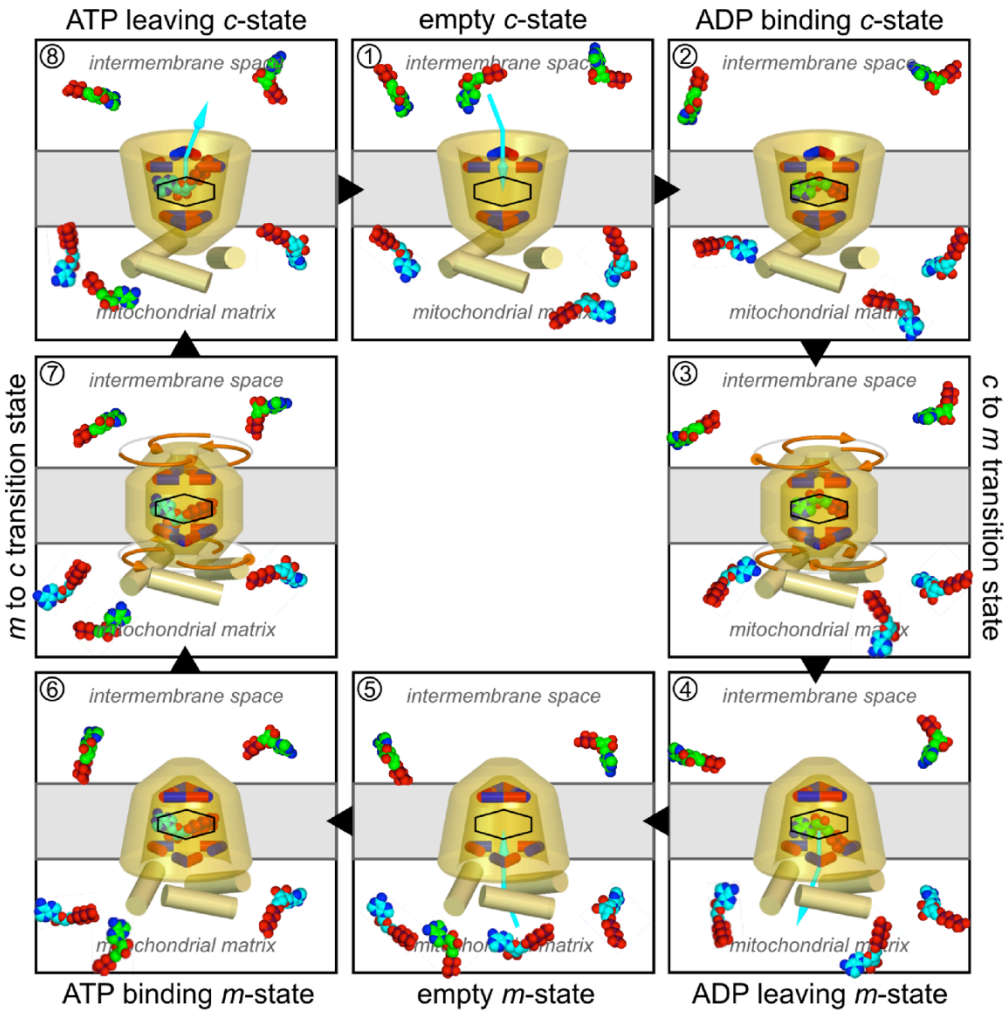

Figure 12 Proposed transport mechanism of the mitochondrial ADP/ATP carrier. Transport cycle of strict equimolar ADP-ATP exchange. Negatively charged and positively charged residues of the salt bridge networks are shown as red and blue sticks, respectively. The imported ADP and exported ATP are green and cyan, respectively. The hexagon indicates the position of the asymmetric substrate binding site. All transport steps are fully reversible, but the direction of transport (black arrow heads) is determined by the membrane potential and by the chemical gradients of ADP and ATP. During substrate import, the matrix network on the odd-numbered α-helices is released whilst the cytoplasmic network on the even-numbered α-helices is formed, and the converse is true during substrate export. The structural changes might occur via a simultaneous twist of the three domains (orange arrows).

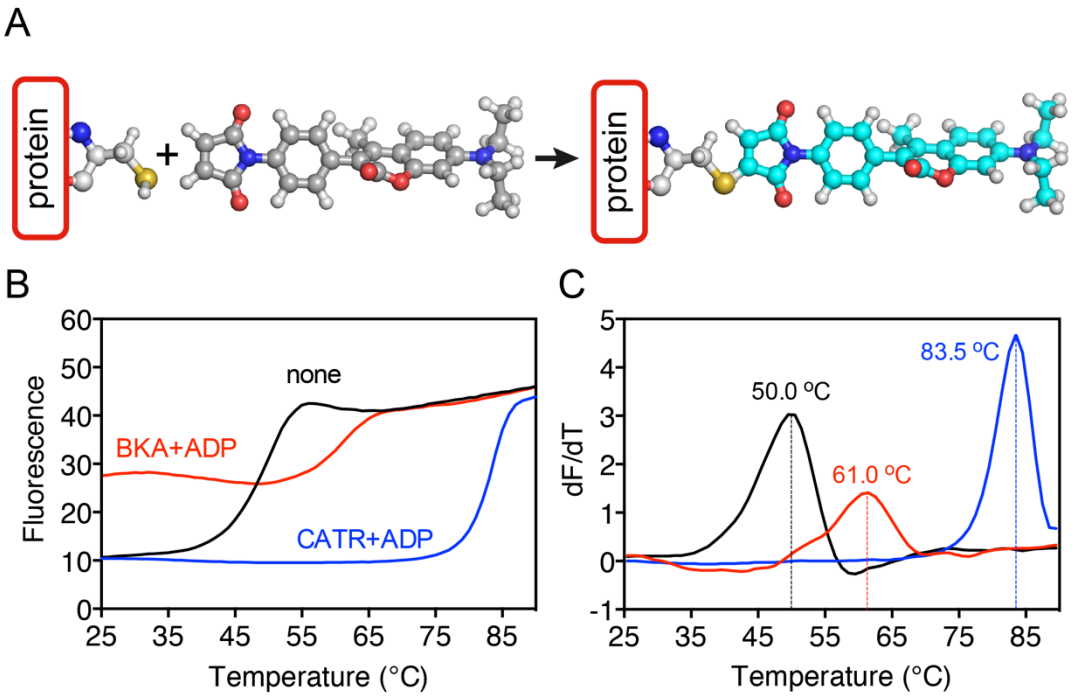

Figure 13 Thermostability of purified wild-type ADP/ATP carrier of *Myceliophthora thermophile* in detergent in the presence of inhibitors and ADP. A The thermostability assay uses the probe CPM, which reacts with exposed protein thiols to form a blue fluorescent adduct [97]. In the procedure, the temperature of purified protein samples is increased from 25 to 90 °C while protein unfolding is monitored with CPM, as buried cysteine residues become solvent exposed due to thermal denaturation of the protein [98]. B Representative unfolding profiles of uninhibited AAC (black line), CATR-inhibited AAC (blue line) and BKA-inhibited AAC (red line) in detergent [96]. The substrate ADP was added to shift the entire population of carriers to the inhibited conformations. C Derivatives of the unfolding profiles in B. The apparent melting temperatures are indicated.

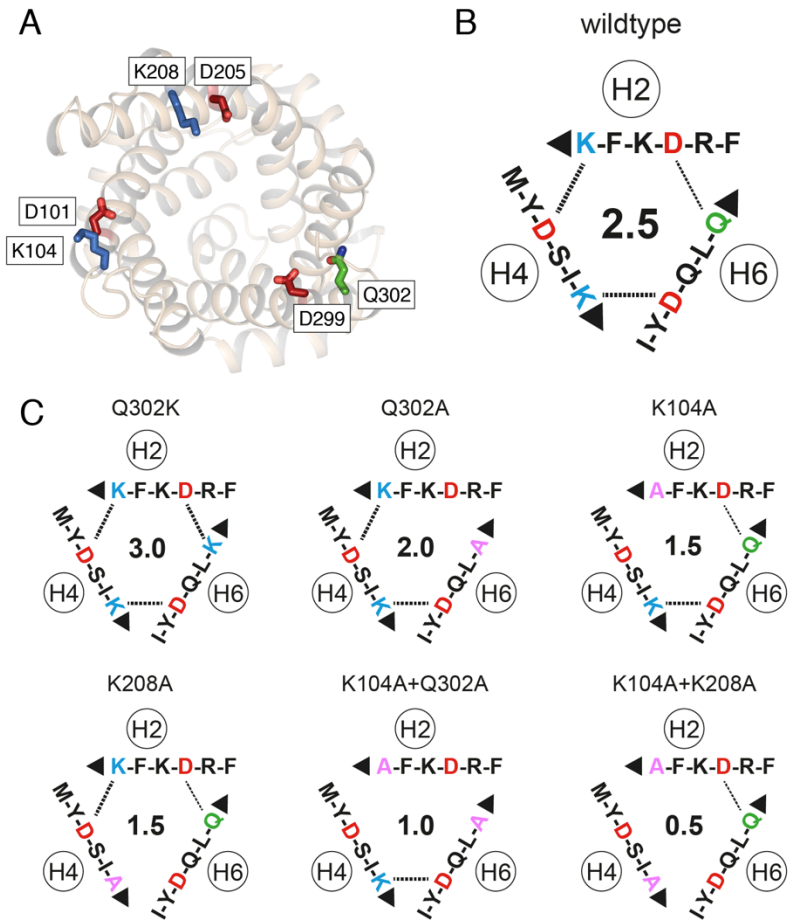

Figure 14 Cytoplasmic salt bridge network of the mitochondrial ADP/ATP carrier (A) View from the intermembrane space/cytoplasm of the comparative homology model of the ADP/ATP carrier of *Myceliophthora thermophile* based on the related structure of Aac2p of *Saccharomyces cerevisiae* (4C9G)[67]. Acidic, basic and polar residues are shown as red, blue and green sticks, respectively. Schematic representations of the cytoplasmic salt bridge network of (B) the wild-type and (C) the cytoplasmic network mutants. The semi-quantitative interaction energy of the

cytoplasmic network is indicated in the centre, in which 1 and 0.5 point are assigned to each salt bridge and hydrogen bond, respectively [92].

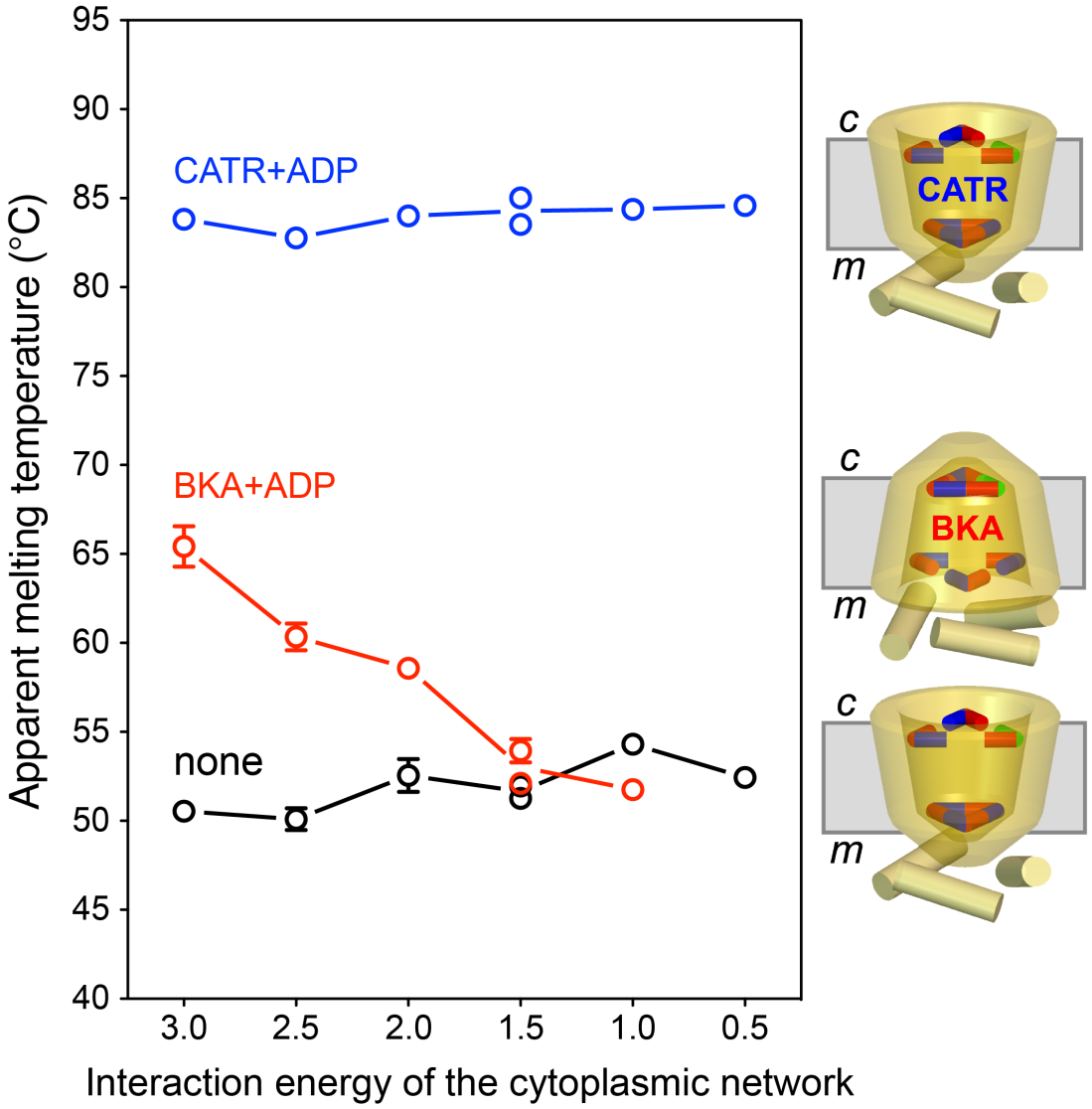

Figure 15 Thermostability of the BKA-inhibited conformation is dependent on the interaction energy of the cytoplasmic network. Apparent melting temperatures of wildtype and mutant were determined in the absence of inhibitor (black) or in the presence of CATR plus ADP (blue) or BKA plus ADP (red) [96]. The double mutant with an interaction energy of 0.5 could not be locked in the BKA-inhibited matrix conformation. The theoretical interaction energy is shown between brackets (see legend to Fig. 1).

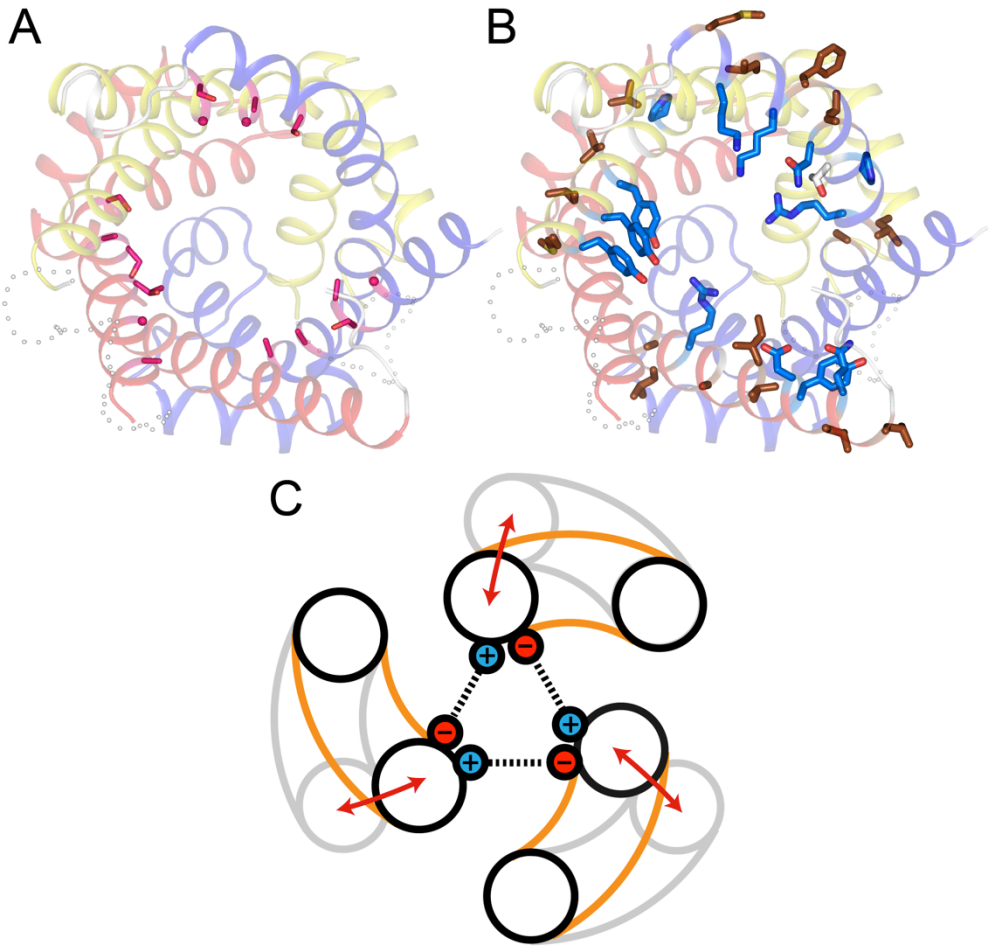

Figure 16 Conserved properties of the inter-domain interfaces suggest a domain-based mechanism of transport. The structure of the yeast ADP/ATP carrier in cartoon representation viewed from the cytoplasmic side [67]. Domain 1, 2 and 3 are coloured blue, yellow, and red, respectively. (A) Residues of the odd-numbered α-helices in the inter-domain interface have no or small side chains, including the residues of the conserved GXXXG motif. (B) Residues of the even-numbered α-helices in the inter-domain interface are mostly either hydrophobic (brown), facing the membrane, or hydrophilic (blue), facing the cavity. (C) Proposed schematic domain motions in the transport cycle [67]. The grey lines represent the helical arrangement in the cytoplasmic conformation, whereas the coloured lines represent the helical arrangement in the matrix conformation. The positive and negatively charged residues of the cytoplasmic salt bridge network are shown in blue and red, respectively. The formation of the cytoplasmic salt bridge network is shown as dashed lines.